THE PENNSYLVANIA STATE UNIVERSITY
SCHREYER HONORS COLLEGE

DEPARTMENT OF MATHEMATICS

ANALYSIS OF THE SIR MODEL ON A NETWORK OF NODES

ISABELLE STEPLER
SPRING 2023

A thesis
submitted in partial fulfillment
of the requirements
for baccalaureate degrees
in Applied and Industrial Mathematics
with honors in Mathematics

Reviewed and approved* by the following:

Pierre-Emmanuel Jabin
Professor of Mathematics
Thesis Supervisor

Diane Henderson
Professor of Mathematics
Honors Adviser

*Signatures are on file in the Schreyer Honors College.

Abstract

The Susceptible-Infected-Recovered model, or SIR model, was one of the first infectious disease models created. Since its first application, it has been modified in many different ways to more accurately model infectious diseases in different situations. This paper explores the standard SIR model, the standard SIR model without lifetime immunity, and the multi-node SIR model in order to investigate the effectiveness and the differences between each model. We analyze the convergence of each model as time approaches infinity, simulate the two-node model to confirm that multi-node SIR models can reproduce multiple infection peaks, and discuss parameter estimation to discover when SIR models, especially on multiple nodes, can be fitted to data and then used for prediction. Due to these investigations, we conclude that multi-node SIR models are a viable option for modeling complicated, real-world disease situations because of their inherent flexibility and ability to reproduce varied infection dynamics. For ideal parameter estimation, multi-node SIR models should only have a few nodes and use data points as spaced out in time as possible, allowing prediction to be more accurate.

Table of Contents

List of Figures

List of Tables

Acknowledgements

This project was supported by the Women in Math Fellowship and the Mathematics Alumni Enhancement Fund for Undergraduates Grant at The Pennsylvania State University.

Special thanks to my wonderful thesis advisor, Pierre-Emmanuel Jabin, for teaching me so much throughout this long project, and to Amina Amassad for all of her support and advising on this project. And my deepest gratitude to all of my mentors in the math department, especially Cheryl Hile, David Nieves, Amine Benkiran, Jessica Conway, and Diane Henderson for their endless support and the opportunities they have given me.

Chapter 1

Introduction

Infectious diseases have always affected populations throughout recorded history, and they will continue to invade populations with unpredictable impacts. Because all infectious diseases have different characteristics, predicting their path through a population is always challenging. Some diseases are short but catastrophic events, such as the Black Death (bubonic plague) in the fourteenth century and the Spanish flu in the beginning of the twentieth century. However, diseases can also become endemic in the population, like measles, malaria, typhus, cholera, tuberculosis, HIV/AIDS, and sleeping sickness, returning annually or constantly to affect millions across the globe. Epidemics cause considerable damage to life span, quality of life, and economic prosperity, especially in developing countries. Thus, so that epidemics can be better treated and protected against in the future, it is crucial for scientists to understand the nature of disease spread. Mathematicians can help answer a crucial epidemiology question: can we model disease spread to determine causes and predict the effects on the population as a whole?

The study of infectious disease data originated with John Graunt's 1662 book "Natural and Political Observations made upon the Bills of Mortality." Using the data from the Bills of Mortality, the weekly records of the death in London parishes, Graunt estimated the risks of death by different diseases. Typically, the first model in mathematical epidemiology is considered to be David Bernoulli's work on inoculation against smallpox in the 1760's. Bernoulli studied the benefits of inoculation by calculating the increase in life expectancy if smallpox was eradicated as a cause of death. In addition to Graunt and Bernoulli, John Snow studied temporal and spatial patterns of cholera cases in the 1855 epidemic in London and used mathematical methods to determine the Broad Street water pump as the source of infection; these same techniques were used for a typhoid outbreak in 1873. [1]

Now in the 21st century, multitudes of data on past and current epidemics exist for scientist and mathematicians to analyze and use to predict future outbreaks. Recent diseases like SARS, H1N1 influenza, Ebola virus, and especially Covid-19 have revived the interest in epidemiological modeling, both theoretically and experimentally. A diverse subject, infectious disease modeling includes several types of model formulation. The first and most famous model is the compartmental model, which will be discussed in detail below. However, because the transmission of infection is intrinsically stochastic, relying on the probabilistic interaction between members of the population, stochastic models of disease have a very important role in epidemiological modeling. For example, a common approach is to describe the beginning of a disease outbreak with a stochastic branching process. A stochastic model for the beginning of the outbreak could also transition to a compartmental model when the mixing of populations is reasonably homogeneous. There has also been a more recent emphasis on network models, a currently rapidly developing field of study in epidemic modeling that this paper will explore in detail and in combination with a compartmental model. Modern problems like drug resistance, multiple sources of infection, and mutation require more complicated models to capture more variable epidemiological situations. [1]

The majority of this paper will discuss a compartmental model for disease spread. In a compartmental model, populations are organized into compartments, where individuals can move between compartments at different rates as they progress through the disease. The foundation of compartmental models lies in the assumption that the spread of infection is caused by microorganisms, the existence of which was shown in 1632 by van Leeuwenhoek; then, the germ theory of disease was created in 1840 by Jacob Henle then expanded upon by scientists such as Robert Koch and Louis Pasteur. The mass action law, another fundamental part of compartmental models, was first applied to epidemiology by W.H. Hamer in 1906 to describe the rate of new infections, which depends on

numbers of both susceptible and infected individuals. Most importantly, public health physicians A.G. McKendrick and W.O. Kermack established the basic infectious disease compartmental models, including the SIR model, in a series of papers from 1927-1933; these models have been used and adapted to study epidemics ever since. [1]

Compartmental models can be either simple, to study general qualitative behavior, or detailed, to model specific situations and produce short-term quantitative predictions. The detailed models are much harder to solve analytically but are more useful for predictions and policy decisions, while simple models are more useful for theoretical purposes. Recently, the advances in high-powered computing have aided the investigations of complicated detailed models. [1]

A common compartmental model for disease spread where the population can either be susceptible, infected, or recovered, the SIR model can be varied in different ways according to the desired disease application. While we will study the standard case and the case where individuals can become reinfected, modifying the SIR model to include more robust temporary immunity, infection delay, and natural births and deaths can adapt the model to different situations.

The goal of this project is to perform analysis on the standard SIR model and the SIR model without lifetime immunity, then to expand the SIR model to a network of nodes, analyze the behavior there, and perform some parameter estimation to gain insight on what conditions lead to complete extinction of the disease. In general, each analysis portion finds the equilibrium points of the system then uses techniques including the dynamical invariant, rescaling, Lyapunov functions, and Gronwall's Lemma to prove convergence to a set of those equilibrium points. Numerical simulation was also used for the SIR model on two nodes to inform that system's analysis. Finally, the analysis of the multi-node SIR model is supplemented with a discussion of parameter estimation.

Through these investigations, we highlight several important similarities and differences between the single-node and multi-node SIR models. Both models show convergence to an epidemic-free state as t approaches ∞. However, the multi-node model needs to be treated more carefully because the analysis becomes more challenging and parameter estimation may fail as the number of nodes increases. Nonetheless, the multi-node model is a natural model for networks of population centers or habitats, and it can capture behavior not modelled in the single-node case, as seen in the numerical simulations of the two-node model. In conclusion, it is most practical to use a model that uses few enough nodes to be able to estimate parameters while still effectively modeling the disease and data.

Chapter 2

Models

This thesis focuses on the Susceptible-Infectious-Recovered (SIR) model for infectious disease in three ways. Each type of model reflects the situation where a disease sweeps through a closed population of individuals on a short time scale (on the order of weeks or months), which allows the assumption that any demographic turnover (births or natural deaths, or immigration and emigration) can be ignored. Until at least one infected individual introduces the disease to the rest of the population, this population is completely free of infection. The analysis of each model strives to deduce what conditions lead to an epidemic and the amount of individuals affected by that epidemic as a whole. These models also assume that the infections are caused by microparasites that are spread by contact between two individuals. These assumptions allow these models to be used and adapted to study the spread of common diseases like influenza, HIV, and very recently, COVID-19, depending on the conditions of the population and contact among its members. [3]

2.1 The Standard SIR Model

The standard SIR model focuses on a population of N individuals that can contract a certain disease one time. The susceptible population is labeled S, the infected population is labeled I, and the recovered population is labeled R. Assume that the susceptible and infected populations interact according to the law of mass action at rate $\beta = \frac{b}{N} > 0$, where b is the constant number of susceptible contacts each infected person has per unit of time. For this model, assume that after recovering, the previously infected individual has lifetime immunity and stays recovered [3]. Thus, we model recovery with the rate $\alpha > 0$, which is the fixed fraction of the infected group that recovers per unit of time, roughly equivalent to the inverse of the length of the infection. See Figure 2.1 below for the compartmental diagram of the standard SIR system.

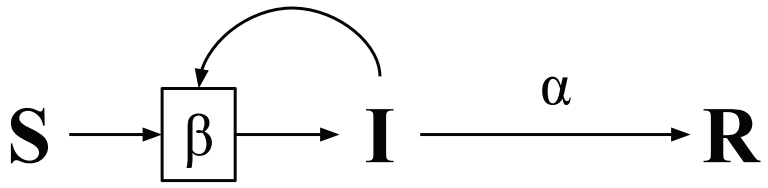

Figure 2.1: Diagram of the SIR Model

For these interactions, the system of differential equations for the standard SIR model is

$$\dot{S} = -\beta SI, \tag{2.1}$$

$$\dot{I} = \beta SI - \alpha I, \tag{2.2}$$

$$\dot{R} = \alpha I. \tag{2.3}$$

It is important to note that these equations do not depend on R, so typically the system is represented using only equations 2.1 and 2.2. In addition, the closed population assumption is

further reinforced by the fact that $\dot{S} + \dot{I} + \dot{R} = 0$, so $S + I + R = N$ must be constant [3]. Since the population is fixed at N individuals, R can be computed as $R = N - S - I$ at any time.

However, the standard SIR model can only be used to model diseases such as chicken pox or measles where individuals cannot become reinfected. So, other diseases that do not give the individual lifetime immunity, like the common cold or COVID-19, cannot be modeled with the standard SIR model. In addition, the standard SIR model does not account for any sort of delay between the time of the individual's infection and the time the individual becomes infectious to others. Finally, a single population is typically connected to other populations, such as a network of towns in a county or herds of a type of grazing animal, but the standard SIR model cannot effectively model these separate connections and their contributions to the spread of infection.

2.2 SIR Model Without Lifetime Immunity

Studying many common infectious diseases means that we cannot always make the assumption that individuals can only be infected once. To reevaluate the SIR model for individuals without lifetime immunity, assume the recovered individuals can now return to the susceptible population and be infected again. Thus, two R terms are added to $\dot{S}$ and $\dot{R}$ in the system of differential equations. The rate $v > 0$ is roughly the inverse of the time of immunity and represents how quickly recovered individuals become susceptible again. All other variables and parameters are the same, and the diagram of the SIR model changes as seen in Figure 2.2 below.

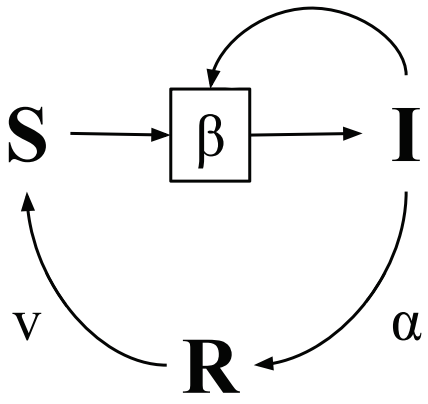

Figure 2.2: Diagram of SIR Model Without Lifetime Immunity

The SIR model without lifetime immunity now has the following updated system of equations:

$$\dot{S} = -\beta SI + vR \tag{2.4}$$

$$\dot{I} = \beta SI - \alpha I \tag{2.5}$$

$$\dot{R} = \alpha I - vR \tag{2.6}$$

The inclusion of the R terms makes analysis of the system more challenging than the standard SIR model while making the model more adaptable to different types of diseases that reinfect individuals. However, the SIR model without lifetime immunity still only considers one population, which is still not quite realistic to how populations interact with each other. Therefore, we can expand the SIR model to a network, as seen in section 2.3.

2.3 SIR Model on Multiple Nodes

The main goal of this project is to extend the standard SIR system from section 2.1 to multiple nodes representing a network of population centers. This network can represent a neighborhood of houses, a state and its counties, or even an entire country and its cities, allowing different population centers to interact at different infection rates. Thus, the SIR model on a network is more adaptable to modeling disease spread through a diverse set of populations and can be made as large or as concentrated as necessary for the specific disease and situation.

A two-node system will be explored for the standard SIR system (back to lifetime immunity) in simulations to model the dynamics of this type of network. Node 1 has susceptible population S_1 and infected population I_1, and node 2 has susceptible population S_2 and infected population I_2, and once again we assume the total population is constant. We can also assume the recovered populations are not necessary to include, as in the model in section 2.1. Now that there are two nodes, the infected populations from each node interact with both of the susceptible populations at different rates, as detailed by Figure 2.3 below, but note that individuals do not move from one node to another. The node 1 infected population interacts with the node 1 susceptible population at rate β_{11} and the node 2 susceptible population at rate β_{21}. Similarly, the node 2 infected population interacts with the node 1 susceptible population at rate β_{12} and the node 2 susceptible population at rate β_{22}. Each β_{ij} and α_i has the same positivity and meaning as described in section 2.1, just characterized to each node.

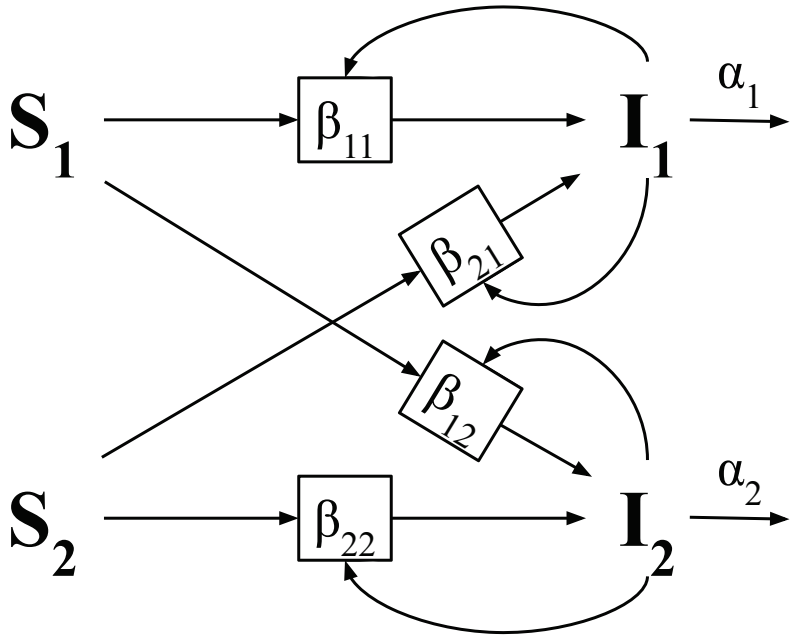

Figure 2.3: Diagram of SIR Model on Two Nodes

The equations for the two-node SIR model are

$$\dot{S}_1 = -\beta_{11} S_1 I_1 - \beta_{12} S_1 I_2, \tag{2.7}$$
$$\dot{S}_2 = -\beta_{21} S_2 I_1 - \beta_{22} S_2 I_2, \tag{2.8}$$
$$\dot{I}_1 = \beta_{11} S_1 I_1 + \beta_{12} S_1 I_2 - \alpha_1 I_1, \tag{2.9}$$
$$\dot{I}_2 = \beta_{21} S_2 I_1 + \beta_{22} S_2 I_2 - \alpha_2 I_2. \tag{2.10}$$

The general system for the SIR model on n nodes, which shares the same assumptions as the two-node model expanded to n nodes, is defined as follows for $i = 1, \ldots, n$:

$$\dot{S}_i = -\left(\sum_{j=1}^{n} \beta_{ij} I_j\right) S_i \tag{2.11}$$
$$\dot{I}_i = \left(\sum_{j=1}^{n} \beta_{ij} I_j\right) S_i - \alpha_i I_i \tag{2.12}$$

While adding nodes creates a more realistic level of complexity for the model, it also adds many parameters that will need to be estimated or analyzed to figure out the behavior of the system.

It can also be useful to use graphs and weighted graphs to describe the multi-node SIR model.

Definition 2.3.1. A **graph** $(V, \mathcal{E})$ is a set of vertices and edges.

Because the network has a finite number of population centers, say n, the set of vertices V will be enumerable. Then the set of edges, $\mathcal{E}$, is a set of pairs of vertex numbers, like (i, j) to denote the edge between the vertices i and j.

Definition 2.3.2. A **weighted graph** associates a weight w_{ij} with an edge (i, j).

Thus, the abstract formulation of the SIR model on n nodes is as follows: on the graph $(V, \mathcal{E}, \omega : \mathcal{E} \to \mathbb{R}^+)$, where ω is the weight function, then for each S_ν, I_ν on each $\nu \in V$,

$$\dot{S}_\nu = -S_\nu \sum_{\nu':(\nu,\nu')\in\mathcal{E}} \omega((\nu, \nu'))I_{\nu'},$$

$$\dot{I}_\nu = S_\nu \left[\sum_{\nu':(\nu,\nu')\in\mathcal{E}} \omega((\nu, \nu'))I_{\nu'} \right] - \alpha_\nu I_\nu.$$

The abstract formulation does not label nodes and hence keeps the generality of the graph. Thus, there can be different weight matrices (up to a permutation) representing the same SIR system graph.

Chapter 3

Analysis on One Node

3.1 Useful Theory

A few theorems and definitions are necessary in order to analyze the systems in the following sections on the SIR model.

Lemma 3.1.1. ***A version of Gronwall's Lemma:*** *Let $X(t) : [0, T] \to \mathbb{R}$ be a nonnegative differentiable function for which there exists a function $C(t)$ and $A(t)$ such that $X'(t) \leq A(t) + C(t)X(t)$. Then*

$$X(t) \leq X_0\, e^{\int_0^t C(s)\,ds} + \int_0^t \left(A(s)\, e^{\int_s^t C(r)\,dr}\right) ds.$$

Proof. Define $X(t) = y(t)\, e^{\int_0^t C(s)\,ds}$. Then

$$X'(t) = y'(t)\, e^{\int_0^t C(s)\,ds} + y(t)C(t)\, e^{\int_0^t C(s)\,ds}.$$

However, because $X'(t) \leq A(t) + C(t)X$,

$$y'(t)\, e^{\int_0^t C(s)\,ds} + y(t)C(t)\, e^{\int_0^t C(s)\,ds} \leq A(t) + C(t)y(t)\, e^{\int_0^t C(s)\,ds},$$

which simplifies to

$$y'(t)\, e^{\int_0^t C(s)\,ds} \leq A(t).$$

Then by solving for $y'(t)$,

$$y'(t) \leq A(t)\ e^{-\int_0^t C(s)\,ds}.$$

After integrating, we find the following equation:

$$y(t) \leq y_0 + \int_0^t A(s)\, e^{-\int_0^s C(r)\,dr}\, ds.$$

Since $y(t) = X(t)\, e^{-\int_0^t C(s)\,ds}$ from our initial definition of $X(t)$ solved for $y(t)$, $y_0 = y(0) = X(0) = X_0$. Therefore, if $y(t)$ is plugged into the definition of $X(t)$,

$$X(t) \leq \left(X_0 + \int_0^t \left(A(s)\, e^{-\int_0^s C(r)\,dr}\right) ds\right) e^{\int_0^t C(s)\,ds},$$

which then implies that

$$X(t) \leq X_0\, e^{\int_0^t C(s)\,ds} + \int_0^t \left(A(s)\, e^{\int_s^t C(r)\,dr}\right) ds.$$

□

Definition 3.1.1. Assume $f : \mathbb{R}^n \to \mathbb{R}^n$ is continuously differentiable, and let $\phi(\cdot, x_0)$ denote the solution of the IVP $\dot{x} = f(x),\ x(0) = x_0$. An equilibrium point x_e of the differential equation is **stable** if given any $\varepsilon > 0$ there is a $\delta > 0$ such that whenever $|x_1 - x_e| < \delta$, the solution $\phi(\cdot, x_1)$ exists on $[0, \infty)$ and for $t \geq 0$,

$$|\phi(t, x_1) - x_e| < \varepsilon.$$

In addition, if there is a $\delta_0 > 0$ such that $|x_1 - x_e| < \delta_0$ implies that

$$\lim_{t\to\infty} \phi(t, x_1) = x_e,$$

then we say that the equilibrium point x_e is **asymptotically stable**. If an equilibrium point is not stable, then it is **unstable**. [4]

Theorem 3.1.2. ***Poincaré-Bendixson Theorem:*** *For $x' = f(x)$, where $x \in \mathbb{R}^n$, and $\phi(t, x)$ is a bounded orbit for $t \geq 0$ and W is its ω-limit set, then either W is a cycle, or, for each $y \in W$, the ω-limit set is a set of onep or more equilibrium points. In other words, the solution converges to a stable equilibrium or a cycle surrounding a certain point as t approaches ∞. [4]*

If S, I, and R are bounded by some quantity, the Poincaré-Bendixson Theorem implies that the system can approach either a stable equilibrium or a limit cycle. One way to find a stable equilibrium is to use Lyapunov functions.

Definition 3.1.2. Let x_e be an equilibrium point for $x' = f(x),\ x \in \mathbb{R}^n$. A continuously differentiable function V defined on an open set $U \subset \mathbb{R}^n$, where $x_e \in U$, is a **Lyapunov function** if the following properties hold: [4]

1. $V(x) > V(x_e)$ for all $x \in U$ such that $x \neq x_e$
2. $\nabla V(x) \cdot f(x) \leq 0$ for all $x \in U$. If the inequality is strict, V is a **strict Lyapunov function**.

In other words, as long as V has a minimum at x_e and satisfies the second condition, then V is a Lyapunov function. Some definitions ([4]) include a statement requiring $V(x_e) = 0$, but this statement can always be made true by adding or subtracting a constant from V, which will not change $\nabla V(x)$.

Theorem 3.1.3. ***Lyapunov's Stability Theorem:*** *If V is a Lyapunov function for $x' = f(x)$ on an open set U containing an equilibrium point x_e, then x_e is stable. If V is a strict Lyapunov function, then x_e is asymptotically stable. [4]*

Therefore, if we find a Lyapunov function for an equilibrium point of our system, that equilibrium is stable. This final theorem is necessary for the convergence theorem of the SIR model without lifetime immunity.

3.2 Asymptotic Analysis of Standard SIR Model

This section will explore the asymptotic behavior of the standard SIR model described in section 2.1. Recall that the R equation can be omitted, so the system is simply

$$\dot{S} = -\beta SI,$$
$$\dot{I} = \beta SI - \alpha I.$$

Lemma 3.2.1. *The equilibrium points of the SIR system are $(0, 0)$ and the line $I = 0$, i.e., $(S, 0)\ \forall S$.*

Proof. To find the equilibrium points of the system, find S and I that make each derivative equal to 0. First, setting $\dot{S} = -\beta SI = 0$ means that either $S = 0$ or $I = 0$. Then, if $\dot{I} = \beta SI - \alpha I = 0$ and $S = 0$, then $-\alpha I = 0$, which means that $I = 0$. Or, if $\beta SI - \alpha I = 0$ and $I = 0$, then S can be any value. Alternatively, if we factor out an I in the $\dot{I}$ equation so that now $I(\beta S - \alpha) = 0$, if $I = 0$, S can be any value, or if $S = \frac{\alpha}{\beta}$, then $I = 0$ (a point which is included on the $I = 0$ line that will be important to the convergence theorem). In conclusion, the equilibrium points are $(0, 0)$ and $(S, 0)\ \forall S$. □

The behavior of the system can also be explored through an implicit solution, found by dividing one of the differential equations by the other to get an equation that does not explicitly rely on time. In the case of the standard SIR model, the implicit solution is also the dynamical invariant of the system.

Definition 3.2.1. A set $S \subseteq \mathbb{R}^n$ is a **invariant set** of a differential equation $\dot{x} = f(x),\ x \in \mathbb{R}^n$, if, for each $x \in S$, the solution $\phi(x)$, defined on its maximum interval of existence, has its image in S. [2]

Thus, the solution to the differential equation maps the invariant set to itself. In other words, if a point is in the invariant set, the solution at that point stays in the invariant set. The dynamical invariant in our case will be the implicit solution, which happens to describe the invariant set.

Lemma 3.2.2. *The implicit solution for the SIR system is* $I = \frac{\alpha}{\beta} \ln \frac{S}{S_0} - S + S_0 + I_0$.

Proof. Here, we can divide dI/dt by dS/dt then use separation of variables:

$$\frac{dI}{dS} = \frac{\beta SI - \alpha I}{-\beta SI} = \frac{\alpha}{\beta}\left(\frac{1}{S}\right) - 1.$$

This equation is separable, so we can move the dS to the other side and integrate both sides as follows:

$$\int_{I_0}^{I} d\gamma = \int_{S_0}^{S} \left(\frac{\alpha}{\beta}\left(\frac{1}{s}\right) - 1\right) ds.$$

Integrating both sides gives

$$I - I_0 = \left(\frac{\alpha}{\beta} \ln |s| - s\right) \Big|_{S_0}^{S},$$

then evaluate the right hand side at S and S_0 (which are both positive, so the absolute value can be dropped):

$$I - I_0 = \frac{\alpha}{\beta} \ln S - S - \left(\frac{\alpha}{\beta} \ln S_0 - S_0\right).$$

Simplifying the equation yields

$$I - I_0 = \frac{\alpha}{\beta}\Big(\ln S - \ln S_0\Big) - S + S_0,$$

and finally, combine the log terms into one term and move I_0 to the other side to get the implicit solution as

$$I = \frac{\alpha}{\beta} \ln \frac{S}{S_0} - S + S_0 + I_0. \tag{3.1}$$

□

Equation 3.1 will be used in later theorems to help determine end behavior for the system.

Definition 3.2.2. The **basic reproduction number**, R_0, is the expected number of new infections from a single infectious individual in a population of all susceptible individuals. [3]

In the standard SIR model, R_0 is, in other words, the average number of contacts by an infectious individual with others before infection is over, represented as $R_0 = \frac{\beta}{\alpha}S$. [3]

See the following theorem for the examination of the standard SIR model's end behavior.

Theorem 3.2.3. *As $t \to \infty$, (S, I) will approach:*

1. *$(\bar{S}, 0)$ where $\bar{S} < S_0$ and I converges monotonically if $S_0 < \frac{\alpha}{\beta}$, or*
2. *$(\bar{S}, 0)$ where $\bar{S} < \frac{\alpha}{\beta}$ and I does not converge monotonically if $S_0 > \frac{\alpha}{\beta}$.*

Proof. There are two ways to prove this theorem. The first is by using the differential equations and separation of variables.

1. Looking at the differential equations, $\dot{S} < 0$, so S will always be decreasing. In addition, since $S_0 < \frac{\alpha}{\beta}$, S will be less than $\frac{\alpha}{\beta}$; thus, $\dot{I} < 0$ as well. Specifically, we know $S \leq \frac{\alpha}{\beta}$ for all time because S is decreasing, so $\dot{I} \leq (\beta S_0 - \alpha)I = -cI$ for some $c > 0$. Therefore, I is approximately decreasing exponentially. Therefore, let $I \leq I_0 e^{-ct}$, so the S equation becomes $\dot{S} = -\beta SI \geq -\beta S I_0 e^{-ct}$. Using separation of variables, we evaluate the integral

$$\int_{S_0}^{S} \left(\frac{1}{s}\right) ds \geq \int_0^t \left(-\beta I_0 e^{-c\tau}\right) d\tau.$$

   Integrating both sides gives

$$\ln S - \ln S_0 \geq \frac{\beta}{c} I_0 (e^{-ct} - 1),$$

   which we then multiply by a negative to get

$$\ln S_0 - \ln S(t) \leq \frac{\beta}{c} I_0 (1 - e^{-ct}).$$

   As $t \to \infty$, then

$$\ln S_0 - \ln S(t) \leq \frac{\beta}{c} I_0.$$

   Thus, by solving for S, S approaches a value

$$\bar{S} \geq S_0 e^{-\frac{\beta}{c} I_0} \neq 0.$$

   However, since S is always decreasing, we know that $\bar{S} < S_0$. Since I decreases approximately exponentially, I decreases monotonically toward 0. Therefore, the result for the first case is proven.

   This result is further illustrated by the graph below. In figure 3.1, I decreases monotonically to 0 as time increases, as just proved ($\alpha = 1, \beta = 1, S_0 = 0.5, I_0 = .25$).

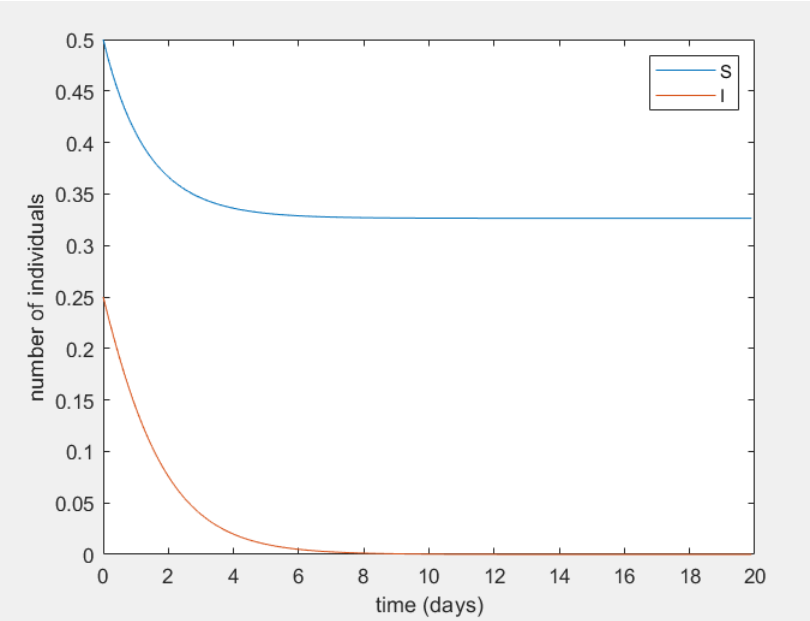

Figure 3.1: S, I as a function of time for $S_0 < \alpha/\beta$

2. By analyzing the differential equations, when $S_0 > \frac{\alpha}{\beta}$, $\dot{I} = (\beta S - \alpha)I > 0$. Thus, I is initially increasing. However, S is always decreasing, so I will increase until S decreases to below $\frac{\alpha}{\beta}$. Then, $\dot{I} \leq -cI$ again and will decrease approximately exponentially (as shown above in the first case) to 0, and S will approach some $\bar{S} < \frac{\alpha}{\beta}$. The graph below (Figure 3.2) demonstrates the increase and subsequent decrease in I that was just proved.

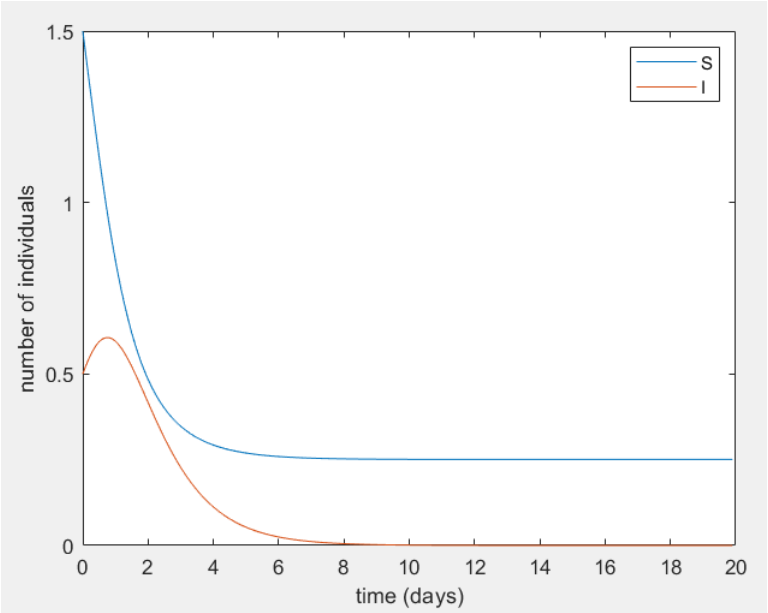

Figure 3.2: S, I as a function of time for $S_0 > \alpha/\beta$

Theorem 3.2.3 can be proved alternatively using the dynamical invariant. Recall the dynamical

invariant equation 3.1, which is

$$I = \frac{\alpha}{\beta} \ln S - S - \frac{\alpha}{\beta} \ln S_0 + S_0 + I_0.$$

Plug the invariant into $\frac{dS}{dt} = -\beta SI$, so the derivative of S becomes

$$\dot{S} = -\beta S\Big(\frac{\alpha}{\beta} \ln S - S - \frac{\alpha}{\beta} \ln S_0 + S_0 + I_0\Big).$$

This new $\dot{S}$ equation can be analyzed to find the limit of S. First, set $\dot{S} = 0$ to find the steady state solutions. The equation $-\beta S(\frac{\alpha}{\beta} \ln S - S - \frac{\alpha}{\beta} \ln S_0 + S_0 + I_0) = 0$ yields

$$\alpha \ln S - \beta S = -\beta S_0 + \beta I_0 + \alpha \ln S_0. \tag{3.2}$$

Define $f(S) = \alpha \ln S - \beta S$ for $S > 0$. The maximum of f occurs at $S = \frac{\alpha}{\beta}$ (set the derivative equal to 0 and solve for S). Thus, for some $y > f(\frac{\alpha}{\beta})$, $f(S) = y$ has no solutions. But for $y < f(\frac{\alpha}{\beta})$, $f(S) = y$ has two solutions S_1 and S_2 on either side of $S = \frac{\alpha}{\beta}$. Let $S_1 < \frac{\alpha}{\beta}$ and $S_2 > \frac{\alpha}{\beta}$.

Therefore, as long as $-\beta S_0 + \beta I_0 + \alpha \ln S_0 < f(\frac{\alpha}{\beta})$, equation 3.2 has two solutions S_1 and S_2, where $S_1 < \frac{\alpha}{\beta}$ and $S_2 > \frac{\alpha}{\beta}$. These solutions S_1 and S_2 are then steady-state solutions of $\dot{S}$. However, because S is always decreasing (because $\dot{S} = -\beta SI$), S must approach $S_1 < \frac{\alpha}{\beta}$. The values of S_1 are different when S_0 is greater than or less than $\frac{\alpha}{\beta}$ (which can be seen in the graphs of the dynamical invariant in fig. 3.3 and fig. 3.4), but S still approaches some positive value less than $\frac{\alpha}{\beta}$. □

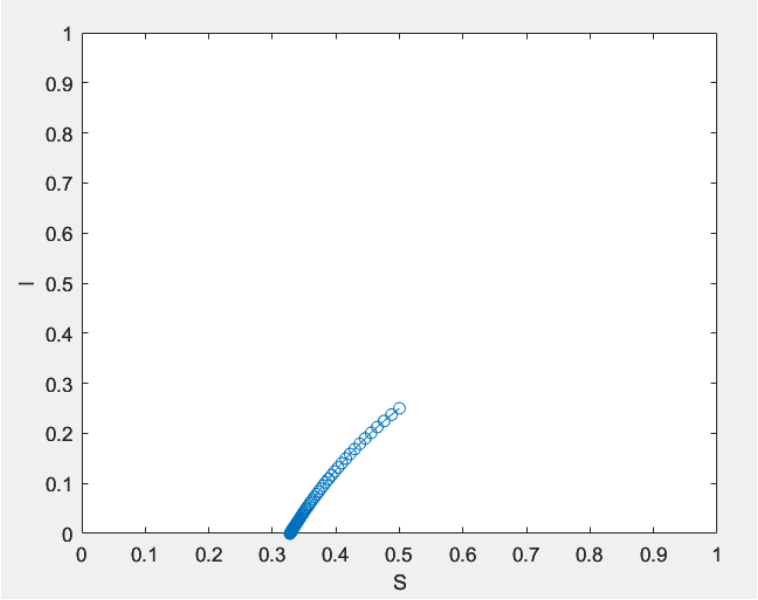

Figure 3.3: Dynamical Invariant for $S_0 < \alpha/\beta$ ($\alpha = 1, \beta = 1$). Under this S_0 condition, I decreases monotonically to 0.

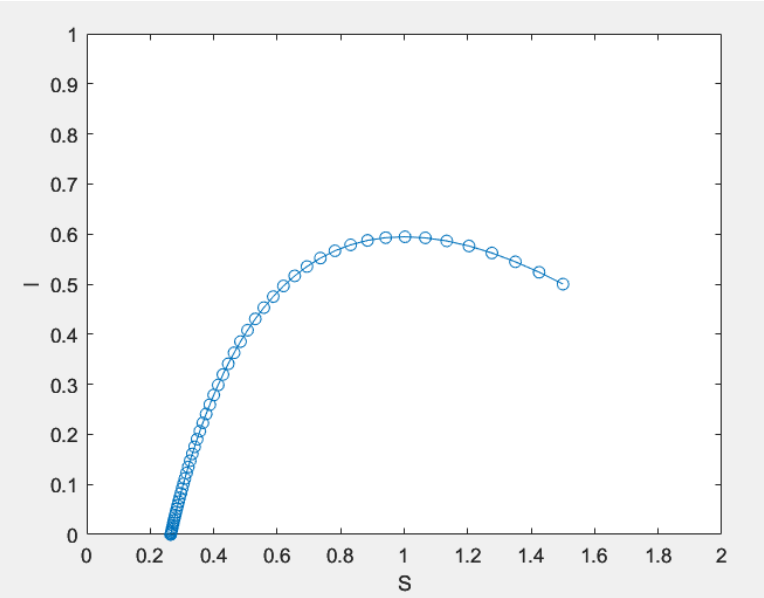

Figure 3.4: Dynamical Invariant for $S_0 > \alpha/\beta$ $(\alpha = 1, \beta = 1)$. Under this S_0 condition, I increases at first, creating an infection peak, then decreases to 0.

Remark 1: The proof with the dynamical invariant only works when the invariant set can be explicitly found for the system. For future SIR systems in this paper, this method of using the invariant will not work, especially for multi-node systems.

Remark 2: Since $R_0 = \frac{\beta}{\alpha}S$, if $S_0 < \frac{\alpha}{\beta}$, then $R_0 < 1$, corresponding to the failure of the system to produce an infection peak. Alternatively, if $S_0 > \frac{\alpha}{\beta}$, then $R_0 > 1$, and the system succeeds in producing an infection peak.

3.3 Analysis of Standard SIR Without Lifetime Immunity

This thesis will now investigate the asymptotic behavior of the standard SIR model without lifetime immunity, as described in Section 2.2. Now, because individuals can become reinfected, meaning that recovered individuals can lose immunity and become susceptible again, the R and S equations have an additional term. Thus, the system is

$$\begin{aligned}\dot{S} &= -\beta SI + vR,\\ \dot{I} &= \beta SI - \alpha I,\\ \dot{R} &= \alpha I - vR.\end{aligned}$$

The analysis of this system is more challenging than the standard SIR model from Section 3.1 due to the additional vR terms. Thus, to reduce the number of parameters and simplify the analysis, we rescale the system. First we create dimensionless variables for all independent and dependent variables:

$$\bar{t} = \frac{t}{t_c},\ \bar{S} = \frac{S}{S_c},\ \bar{I} = \frac{I}{I_c},\ \bar{R} = \frac{R}{R_c},$$

where t_c, S_c, I_c, and R_c are characteristic values of each variable to be determined later.

Second, we re-derive the model using only the dimensionless variables. By substitution and chain rule, we derive the following system

$$\begin{aligned}\frac{d\bar{S}}{d\bar{t}} &= -\beta t_c I_c \bar{S}\bar{I} + \frac{vR_c t_c}{S_c}\bar{R},\\ \frac{d\bar{I}}{d\bar{t}} &= \beta t_c S_c \bar{S}\bar{I} - \alpha t_c \bar{I},\\ \frac{d\bar{R}}{d\bar{t}} &= \frac{\alpha t_c I_c}{R_c}\bar{I} - v t_c \bar{R},\end{aligned}$$

where $\bar{S}(0) = S_0/S_c$, $\bar{I}(0) = I_0/I_c$, and $\bar{R}(0) = R_0/R_c$.

Now that we have this model, we choose to make the S and I coefficients 1 (there is no way to rescale again to get all coefficients equal to 1). Therefore, we let $t_c = 1/\alpha$, and $S_c = I_c = R_c = \frac{1}{t_c\beta} = \frac{\alpha}{\beta}$. These values imply that our system becomes

$$\frac{d\bar{S}}{d\bar{t}} = -\bar{S}\bar{I} + \frac{v}{\alpha}\bar{R}, \tag{3.3}$$

$$\frac{d\bar{I}}{d\bar{t}} = \bar{S}\bar{I} - \bar{I}, \tag{3.4}$$

$$\frac{d\bar{R}}{d\bar{t}} = \bar{I} - \frac{v}{\alpha}\bar{R}. \tag{3.5}$$

For simplicity, we will drop the bar from $\bar{t}$ going forward. We can still assume the conservation $\bar{K} = \bar{S} + \bar{I} + \bar{R}$, so $\bar{K} = \frac{\beta}{\alpha}(S + I + R) = \frac{\beta}{\alpha}K$. For the following analysis, the rescaled system can be reduced to two variables by rewriting the conservation equation as $\bar{R} = \bar{K} - \bar{S} - \bar{I}$. Therefore, equations (3.3) and (3.4) become

$$\frac{d\bar{S}}{dt} = -\bar{S}\bar{I} + \frac{v}{\alpha}(\bar{K} - \bar{S} - \bar{I}), \tag{3.6}$$

$$\frac{d\bar{I}}{dt} = \bar{S}\bar{I} - \bar{I}. \tag{3.7}$$

Therefore, this rescaled system only has two parameters now: $\frac{v}{\alpha}$ and $\bar{K}$. We begin the analysis of the rescaled system with the identification of the system's equilibrium points.

Lemma 3.3.1. *The equilibrium points of the system of equations (3.6) and (3.7) are* $(\bar{K}, 0)$ *and* $\left(1, \frac{v(\bar{K}-1)}{\alpha+v}\right)$.

Proof. Set both $\frac{d\bar{S}}{dt} = 0$ and $\frac{d\bar{I}}{dt} = 0$. Then $\frac{d\bar{I}}{dt} = \bar{I}(\bar{S} - 1) = 0$, so either $\bar{I} = 0$ or $\bar{S} = 1$.

If $\bar{I} = 0$, then $\frac{d\bar{S}}{dt} = 0$ yields $\frac{v}{\alpha}(\bar{K} - \bar{S} - 0) = 0$, so since $\frac{v}{\alpha} \neq 0$, then $\bar{S} = \bar{K}$. Thus, one equilibrium point of the system is $(\bar{K}, 0)$.

If $\bar{S} = 1$, then $\frac{d\bar{S}}{dt} = 0$ yields $(-1)\bar{I} + \frac{v}{\alpha}(\bar{K} - 1 - \bar{I}) = 0$. Thus, the equation becomes $\frac{v}{\alpha}(\bar{K} - 1) = \bar{I}(1 + \frac{v}{\alpha})$, which implies that

$$\bar{I} = \frac{v(\bar{K} - 1)}{\alpha + v}.$$

Therefore, the other equilibrium point of the system is $\left(1, \frac{v(\bar{K}-1)}{\alpha+v}\right)$. □

Note that if $\bar{K} < 1$, then $\frac{v(\bar{K}-1)}{\alpha+v}$ becomes negative, and if $\bar{K} > 1$, then $\frac{v(\bar{K}-1)}{\alpha+v}$ stays positive. Thus, because the equilibrium points change with $\bar{K}$, the behavior of the system is different depending on $\bar{K}$'s value.

Theorem 3.3.2. *As $t \to \infty$, $(\bar{S}, \bar{I})$ will approach:*

1. $(\bar{K}, 0)$ *if* $\bar{K} < 1$, *or*
2. $\left(1, \frac{v(\bar{K}-1)}{\alpha+v}\right)$ *if* $\bar{K} > 1$.

Proof. 1. If $\bar{K} < 1$, then $\bar{S} \leq \bar{K} < 1$ for all t, which also implies that $\frac{d\bar{I}}{dt} = \bar{I}(\bar{S} - 1) < \bar{I}(\bar{K} - 1)$. And, $\bar{K} - 1 < 0$, so $\bar{I}$ is decreasing approximately exponentially. So, we find that, in a similar way to part 1 of the proof of Theorem 3.1.3, $\bar{I} \leq \bar{I}_0\, e^{-(1-\bar{K})t}$; therefore, $\bar{I}$ will approach 0 as $t \to \infty$.

Then, look at $\frac{d\bar{R}}{dt} = \bar{I} - \frac{v}{\alpha}\bar{R}$. Since $\bar{I}$ is decreasing approximately exponentially, i.e. $\bar{I} \leq \bar{I}_0\, e^{-(1-\bar{K})t}$,

$$\frac{d\bar{R}}{dt} \leq \bar{I}_0\, e^{-(1-\bar{K})t} - \frac{v}{\alpha}\bar{R}.$$

Since $\frac{d\bar{R}}{dt} \leq A(t) + C(t)\bar{R}$, where $A(t) = \bar{I}_0\, e^{-(1-\bar{K})t}$ and $C(t) = -\frac{v}{\alpha}$, Gronwall's Lemma can be applied here to find that

$$\bar{R} \leq \bar{R}_0\, e^{-\frac{v}{\alpha}t} + \int_0^t \left(\bar{I}_0\, e^{-(1-\bar{K})s}\, e^{-\frac{v}{\alpha}(t-s)}\right) ds.$$

Then simplify the exponential within the integral to get

$$\bar{R} \leq \bar{R}_0\, e^{-\frac{v}{\alpha}t} + e^{-\frac{v}{\alpha}t} \int_0^t \left(\bar{I}_0\, e^{(\frac{v}{\alpha}-1+\bar{K})s}\right) ds,$$

and from there we integrate to find that

$$\bar{R} \leq \bar{R}_0\, e^{-\frac{v}{\alpha}t} + \frac{\bar{I}_0}{\frac{v}{\alpha} + \bar{K} - 1}\left(e^{(\bar{K}-1)t} - e^{-\frac{v}{\alpha}t}\right).$$

Because $\bar{K} < 1$, $\bar{R}$ is decreasing exponentially; therefore, as $t \to \infty$, $\bar{R} \to 0$.

Hence, because $\bar{I}, \bar{R} \to 0$ as $t \to \infty$ and $\bar{S} + \bar{I} + \bar{R} = \bar{K}$, $\bar{S} \to \bar{K}$. Therefore, $(\bar{S}, \bar{I}) \to (\bar{K}, 0)$ as $t \to \infty$ if $\bar{K} < 1$.

2. If $\bar{K} > 1$, the analysis cannot use the same strategies as for $\bar{K} < 1$. However, because $\bar{S}$, $\bar{I}$, and $\bar{R}$ are all bounded by $\bar{K}$, the Poincaré-Bendixson Theorem demonstrates that the rescaled system will either approach a stable equilibrium or a limit cycle.

We try to find a Lyapunov function that works for $\left(1, \frac{v(\bar{K}-1)}{\alpha+v}\right)$. First, note that

$$\frac{d}{dt}(\ln \bar{I}) = \frac{1}{\bar{I}}\left(\frac{d\bar{I}}{dt}\right) = \frac{1}{\bar{I}}(\bar{I}(\bar{S} - 1) = \bar{S} - 1.$$

Then do a change of variables, where

$$X = \ln \bar{I}, \tag{3.8}$$
$$V = \bar{S} - 1. \tag{3.9}$$

So $\dot{X} = V$, and $\dot{V} = \frac{d(\bar{S}-1)}{dt} = \frac{d\bar{S}}{dt} = -\bar{S}\bar{I} + \frac{v}{\alpha}(\bar{K} - \bar{S} - \bar{I})$. Manipulating this equation by adding 0 in clever ways gives

$$\dot{V} = -\bar{S}\bar{I} + \bar{I} - \bar{I} + \frac{v}{\alpha}(\bar{K} - \bar{S} + 1 - 1 - \bar{I}),$$

which leads to

$$\dot{V} = -\bar{I}(\bar{S} - 1) - \bar{I} + \frac{v}{\alpha}(\bar{K} - 1 - \bar{I}) - \frac{v}{\alpha}(\bar{S} - 1).$$

Then, using the definitions of $V = \bar{S} - 1$, the equation becomes

$$\dot{V} = -V\bar{I} - \bar{I} + \frac{v}{\alpha}(\bar{K} - V - 1 - \bar{I}).$$

Finally,

$$\dot{V} = -V\Big(\bar{I} + \frac{v}{\alpha}\Big) + \frac{v}{\alpha}\bar{K} - \frac{v}{\alpha} - \Big(1 + \frac{v}{\alpha}\Big)\bar{I}.$$

Here, note that because $X = \ln \bar{I},\ \bar{I} = e^X$. Thus, the final equation for $\dot{V}$ is

$$\dot{V} = -V(e^X + \frac{v}{\alpha}) + \frac{v}{\alpha}(\bar{K} - 1) - (1 + \frac{v}{\alpha})e^X,$$

and we have a new system:

$$\dot{X} = V, \tag{3.10}$$
$$\dot{V} = -V\Big(e^X + \frac{v}{\alpha}\Big) + \frac{v}{\alpha}(\bar{K} - 1) - \Big(1 + \frac{v}{\alpha}\Big)e^X. \tag{3.11}$$

We do this change of variables because this new system looks like a physical position-velocity system. Therefore, $\dot{V}$ represents a sum of forces. Denote $c(X) = e^X + \frac{v}{\alpha}$ (and note that $c(X) > 0$ for all X), and let friction be $-Vc(X)$, the first term in $\dot{V}$. The last two terms represent $-P'(X)$, where $P(X)$ is the potential. So, let $-P'(X) = \frac{v}{\alpha}(\bar{K} - 1) - (1 + \frac{v}{\alpha})e^X$, implying the potential is

$$P(X) = -\frac{v}{\alpha}(\bar{K} - 1)X + \Big(1 + \frac{v}{\alpha}\Big)e^X.$$

Because this set of equations now can represent a physical system, this system has a certain energy $E(X, V) = \frac{1}{2}V^2 + P(X)$, i.e., the sum of the kinetic and potential energies.

Note that $\dot{E}(X, V) = \nabla E(X, V) \cdot \langle \dot{X}, \dot{V} \rangle$ by chain rule, so

$$\dot{E}(X, V) = \langle P'(X), V \rangle \cdot \langle V, -Vc(X) - P'(X) \rangle.$$

Thus,

$$\dot{E}(X, V) = -V^2 c(X) \leq 0,$$

because $c(X) > 0$ for all X.

Substitute equations (3.8) and (3.9) into $E(X, V)$ to get the equation back in terms of $\bar{S}$ and $\bar{I}$, and choose it as our Lyapunov function $V(\bar{S}, \bar{I})$:

$$V(\bar{S}, \bar{I}) = \frac{1}{2}(\bar{S} - 1)^2 - \frac{v}{\alpha}(\bar{K} - 1)\ln \bar{I} + \Big(1 + \frac{v}{\alpha}\Big)\bar{I}. \tag{3.12}$$

To verify $V(\bar{S}, \bar{I})$ is a Lyapunov function, show that $V(\bar{S}, \bar{I})$ has a minimum at the equilibrium point, as required by definition 3.1.2. To prove this minimum, let $V(\bar{S}, \bar{I}) = g(\bar{S}) + h(\bar{I})$, where $g(\bar{S}) = \frac{1}{2}(\bar{S} - 1)^2$ and $h(\bar{I}) = -\frac{v}{\alpha}(\bar{K} - 1)\ln \bar{I} + (1 + \frac{v}{\alpha})\bar{I}$. Thus, the minimum of $V(\bar{S}, \bar{I})$ occurs where both $g(\bar{S})$ and $h(\bar{I})$ have minima, if those minima exist.

The minimum of $g(\bar{S})$ may occur where $g'(\bar{S}) = \bar{S} - 1 = 0$, which means $\bar{S} = 1$ is a possible minimum. Then by the second derivative test, where $g''(\bar{S}) = 1 > 0 \,\forall\, \bar{S}$, $\bar{S} = 1$ is the minimum of $g(\bar{S})$.

The minimum of $h(\bar{I})$ may occur where $h'(\bar{I}) = -\frac{v(\bar{K}-1)}{\alpha \bar{I}} + 1 + \frac{v}{\alpha} = 0$. If we move the first term to the other side, the equation becomes

$$\frac{v}{\alpha}\left(\frac{\bar{K} - 1}{\bar{I}}\right) = 1 + \frac{v}{\alpha}.$$

Multiplying by α gives

$$\frac{v(\bar{K} - 1)}{\bar{I}} = \alpha + v,$$

So by switching $\bar{I}$ and $\alpha + v$, we see

$$\bar{I} = \frac{v(\bar{K} - 1)}{\alpha + v},$$

so this value of $\bar{I}$ is a possible minimum. By the second derivative test, where $h''(\bar{I}) = \frac{v}{\alpha}\big(\frac{\bar{K}-1}{\bar{I}^2}\big) > 0 \,\forall\, \bar{I}$, $\bar{I} = \frac{v(\bar{K}-1)}{\alpha+v}$ is the minimum for $h(\bar{I})$.

Hence, the minimum of $V(\bar{S}, \bar{I})$ occurs at the equilibrium point $\big(1, \frac{v(\bar{K}-1)}{\alpha+v}\big)$, as required. A constant can be added or subtracted to $V(\bar{S}, \bar{I})$ to ensure that the minimum value is 0.

Therefore, we have proved that $V(\bar{S}, \bar{I})$ is a Lyapunov function for the equilibrium point $\big(1, \frac{v(\bar{K}-1)}{\alpha+v}\big)$, so this equilibrium point is Lyapunov stable. Thus, if $\bar{K} > 1$, as $t \to \infty$, $(\bar{S}, \bar{I}) \to \big(1, \frac{v(\bar{K}-1)}{\alpha+v}\big)$.

□

Since the rescaled system is equivalent to the SIR system without lifetime immunity given at the beginning of Section 3.2, the equilibrium points and convergence behavior of both systems are also equivalent. If desired, one can convert the rescaled system and its equilibrium points back to the original SIR system without lifetime immunity by using the dimensionless variable equations with the chosen characteristic variable values.

Chapter 4

Analysis on Multiple Nodes

4.1 Analysis of the SIR Model on n Nodes

Here we investigate the asymptotic behavior of the standard SIR model on n nodes discussed in section 2.3. Recall that the SIR system on n nodes is as follows (with lifetime immunity once again) for $i = 1, \ldots, n$:

$$\dot{S}_i = -\left(\sum_{j=1}^{n} \beta_{ij} I_j\right) S_i, \tag{4.1}$$

$$\dot{I}_i = \left(\sum_{j=1}^{n} \beta_{ij} I_j\right) S_i - \alpha_i I_i. \tag{4.2}$$

Lemma 4.1.1. *The equilibrium points of the system of equations (4.1)-(4.2) are* $(S_1, \ldots, S_n, 0, \ldots, 0)$ $\forall\ S_1, \ldots S_n \geq 0$.

Proof. First, set $\dot{S}_i$ and $\dot{I}_i$ equal to 0 $\forall\ i = 1, \ldots, n$. If we manipulate the equations a bit, we get the following two equations for each $i = 1, \ldots, n$:

$$-S_i(\beta_{i1} I_1 + \beta_{i2} I_2 + \ldots + \beta_{in} I_n) = 0, \tag{4.3}$$

$$I_i(\beta_{ii} S_i - \alpha_i) + \left[\sum_{j \neq i} \beta_{ij} I_j\right] S_i = 0. \tag{4.4}$$

Looking at equation (4.3), then either of the following is true: $S_i = 0$ or $I_1 = I_2 = \ldots = I_n = 0$ because we assume $\beta_{ij} > 0$ for all $i = 1, \ldots, n$ and $j = 1, \ldots, n$.

If $S_i = 0$, then equation (4.4), which represents $\dot{I}_i = 0$, becomes $-\alpha_i I_i = 0$. Since α_i is assumed to be positive, then we have $I_i = 0$ as well. However, if $I_1 = I_2 = \ldots = I_n = 0$, then S_i can be anything.

Since this system has a total of $2n$ equations, setting $\dot{S}_i$ and $\dot{I}_i$ equal to 0 yields various combinations of equilibrium points where S_i may or may not be 0 for any $i = 1, \ldots, n$, but $I_i = 0$ for all $i = 1, \ldots, n$. Thus, the set of equilibrium points is $\{(S_1, S_2, \ldots, S_n, 0, 0, \ldots, 0)$ $| \ S_i \geq 0 \ \forall\ i = 1, \ldots, n\}$. □

Now, the goal is to show that the SIR system on n nodes converges to an equilibrium without infection, meaning that I_1, I_2, ..., I_n are zero as time approaches infinity - the infection will die out.

Theorem 4.1.2. *The SIR model on n nodes converges to an epidemic-free equilibrium; in other words, as $t \to \infty$, $(S_1, S_2, \ldots, S_n, I_1, I_2, \ldots, I_n) \to (S_{1_\infty}, S_{2_\infty}, \ldots, S_{n_\infty}, 0, \ldots, 0)$ where $S_{1\infty}$, $S_{2\infty}$, ..., $S_{n_\infty} > 0$.*

Proof. First, let $S = S_1 + S_2 + \ldots + S_n$ be the total susceptible population across both nodes and $I = I_1 + I_2 + ... + I_n$ be the total infection population across both nodes.

Second, introduce numbers $\bar{\beta}$ and $\underline{\beta}$ such that for $i = 1, \ldots, n$ and $j = 1, \ldots, n$, $\underline{\beta} \leq \beta_{ij} \leq \bar{\beta}$. Then, we see that $\dot{S} = \dot{S}_1 + \dot{S}_2 + \ldots + \dot{S}_n$. Note that

$$\dot{S}_1 + \dot{S}_2 + \ldots + \dot{S}_n \leq -\underline{\beta}\left(S_1 \sum_{j=1}^{n} I_j + S_2 \sum_{j=1}^{n} I_j + \ldots + S_n \sum_{j=1}^{n} I_j \right) = -\underline{\beta} SI.$$

Thus, if we do the same process with $\bar{\beta}$, we find

$$-\bar{\beta} SI \leq \dot{S} \leq -\underline{\beta} SI. \tag{4.5}$$

In addition, introduce numbers $\bar{\alpha}$ and $\underline{\alpha}$ such that for $i = 1, \ldots, n$, $\underline{\alpha} \leq \alpha_i \leq \bar{\alpha}$. Now, because $\dot{I} = \dot{I}_1 + \dot{I}_2 + \ldots + \dot{I}_n$, and

$$\dot{I}_1 + \dot{I}_2 + \ldots + \dot{I}_n \leq \bar{\beta}\left(S_1 \sum_{j=1}^{n} I_j + S_2 \sum_{j=1}^{n} I_j + \ldots + S_n \sum_{j=1}^{n} I_j \right) - \underline{\alpha} \sum_{j=1}^{n} I_j,$$

we find by the same process as with $\dot{S}$ that

$$\underline{\beta} SI - \bar{\alpha} I \leq \dot{I} \leq \bar{\beta} SI - \underline{\alpha} I. \tag{4.6}$$

Assume that I does not go to 0 initially; however, S is always decreasing, so I will eventually start to decrease. Recall that the equilibrium points for the standard SIR model are $(S, I) = (S, 0)$ $\forall\, S \geq 0$, and the end behavior changes at $S = \frac{\alpha}{\beta}$ according to Theorem 3.1.3. In the SIR system on n nodes that is simplified into $S = S_1 + \ldots + S_n$ and $I = I_1 + \ldots + I_n$, instead of $\frac{\alpha}{\beta}$, we look at S_∞, the limit of S as $t \to \infty$. We investigate whether S_∞ is above or below $\underline{\alpha}/\bar{\beta}$, which is the smallest fraction created from either $\underline{\alpha}$ or $\bar{\alpha}$ divided by either $\underline{\beta}$ or $\bar{\beta}$.

If $S_\infty < \underline{\alpha}/\bar{\beta}$, then as t approaches ∞, $\dot{I} \leq (\bar{\beta} S - \underline{\alpha}) I \leq -cI$ for some real number $c > 0$. Thus, using the same strategy as in Theorem 3.1.3, we conclude that $I \leq I_0 e^{-ct}$, so $I \to 0$ as $t \to \infty$, and S approaches some $S_\infty > 0$ as $t \to \infty$. Since $I = I_1 + \ldots + I_n$, then

$$\dot{I} \leq -cI = -c \sum_{i=1}^{n} I_i.$$

Therefore, I_i for all $i = 1, \ldots, n$ also decrease approximately exponentially to 0 as $t \to \infty$ because $I_i \leq I_0 e^{-ct}$ $\forall\, i = 1, \ldots, n$. In addition, because $\dot{S}_i \geq -\bar{\beta} S_i I$ for all $i = 1, \ldots, n$ and $I \to 0$ as $t \to \infty$, $\dot{S}_i \geq 0$ as $t \to \infty$ for all $i = 1, \ldots, n$. Thus, $S_i \to S_{i_\infty} > 0$ for all $i = 1, \ldots, n$ as $t \to \infty$.

Otherwise, if $S_\infty \geq \underline{\alpha}/\bar{\beta}$, we first want to prove that $I = I_1 + \ldots + I_n$ approaches 0 as $t \to \infty$. Because $S_\infty \geq \underline{\alpha}/\bar{\beta}$,, then $S \geq \underline{\alpha}/\bar{\beta}$ for all t. We also know that $\dot{S} \leq -\underline{\beta} SI$; thus, we can solve for S by separation of variables. First, move all S terms to the same side:

$$\frac{dS}{S} \leq -\underline{\beta} I \, dt.$$

Then, integration yields

$$\ln \frac{S}{S_0} \leq -\underline{\beta} \int_0^t I(s) \, ds.$$

We can further conclude that

$$\ln \frac{\underline{\alpha}}{\bar{\beta} S_0} \leq -\underline{\beta} \int_0^t I(s)\, ds.$$

Thus, the above equation implies that

$$\int_0^t I(s)\, ds \leq -\frac{1}{\underline{\beta}} \ln \frac{\underline{\alpha}}{\bar{\beta} S_0},$$

which proves that $\int_0^t I(s)\, ds$ is bounded uniformly in t and is finite.

We show that I converges to 0 by contradiction: assume that $I(t)$ does not converge to 0 as $t \to \infty$. Then by the converse of the definition of a limit, there exists $\varepsilon > 0$ such that for all $T > 0$, there exists $t > T$ such that $|I(t)| < \varepsilon$. Thus, there is a sequence $t_n \to \infty$ as $n \to \infty$ such that $|I(t_n)| > \varepsilon$. The short proof by induction for this statement is as follows: if t_n exists such that $|I(t_n)| > \varepsilon$, then take $T = 2t_n$, and there exists a $t_{n+1} > T$ such that $|I(t_{n+1})| > \varepsilon$. Clearly $t_{n+1} \geq t_n$, so $t_n \to \infty$ as $n \to \infty$. Next, because $\dot{I} \leq \bar{\beta} S I - \underline{\alpha} I$, we can say $|I'(t)| \leq c$, which implies that $|I(t) - I(\gamma)| \leq c|t - \gamma|$. Then on the interval $[t_n - \delta, t_n + \delta]$, where $\delta = \frac{\varepsilon}{2c}$, $|I(t)| > \varepsilon$. Finally, consider $\int_0^\infty I(t)\, dt$:

$$\int_0^\infty I(t)\, dt \geq \sum_n \int_{t_n - \delta}^{t_n + \delta} I(t)\, dt,$$

The above equation implies that, by average value,

$$\int_0^\infty I(t)\, dt \geq \sum_n \frac{\varepsilon}{2} |t_n + \delta - t_n + \delta|.$$

Thus,

$$\int_0^\infty I(t)\, dt \geq \sum_n \frac{\varepsilon}{2} (2\delta) = \infty,$$

a contradiction with the fact that $I(t)$ has a finite $\int_0^\infty I(t)\, dt$. Thus, I must converge to 0 as $t \to \infty$.

However, this proof that I converges to 0 does not include a rate of convergence, so each I_i could technically converge very slowly to 0, so we cannot use the same strategy as the first case. To better prove convergence for S_i, we use Gronwall's Lemma on the equation $\dot{S}_i \geq -\bar{\beta} S_i I$. Let $C(t) = -\bar{\beta} I(t)$, and $A(t) = 0$. Then we can use the same logical process as the proof of Gronwall's Lemma to show that because $S_i'(t) \geq C(t) S_i(t)$, then

$$S_i(t) \geq S_{i_0} e^{\int_0^t -\bar{\beta} I(s)\, ds} = S_{i_0} e^{-\bar{\beta} \int_0^t I(s)\, ds}.$$

If we take the limit as t approaches ∞, letting the limit of $S_i(t)$ be some value S_{i_∞}, then

$$S_{i_\infty} \geq S_{i_0} e^{-\bar{\beta} \int_0^\infty I(s)\, ds}.$$

Because we have proved that $\int_0^\infty I(t)\, dt$ is finite, the right hand side of this inequality is positive. Therefore, we conclude that as $t \to \infty$, $S_i(t)$ approaches a positive limit S_{i_∞} for all $i = 1, \ldots, n$ as $t \to \infty$.

Therefore, we conclude that as $t \to \infty$, $(S_1, \ldots, S_n, I_1, \ldots, I_n) \to (S_{1_\infty}, \ldots, S_{n_\infty}, 0, \ldots, 0)$ where S_{i_∞} is positive for all $i = 1, \ldots, n$. $\square$

4.2 Simulations of the Two-Node SIR Model

Recall from section 2.3 that the two-node SIR model is given by the following equations:

$$\dot{S}_1 = -\beta_{11} S_1 I_1 - \beta_{12} S_1 I_2, \tag{4.7}$$
$$\dot{S}_2 = -\beta_{21} S_2 I_1 - \beta_{22} S_2 I_2, \tag{4.8}$$
$$\dot{I}_1 = \beta_{11} S_1 I_1 + \beta_{12} S_1 I_2 - \alpha_1 I_1, \tag{4.9}$$
$$\dot{I}_2 = \beta_{21} S_2 I_1 + \beta_{22} S_2 I_2 - \alpha_2 I_2. \tag{4.10}$$

The main goals of the simulations for this model are to illustrate the analysis and end behavior of the system and investigate whether creating an SIR system on two nodes allows multiple infection peaks due to cross-contamination. To numerically solve the system of equations above, I used MATLAB and the forward Euler method (followed by the ode45 solver to check). The set of parameters that varies in the model is $\{\beta_{11}, \beta_{12}, \beta_{21}, \beta_{22}, \alpha_1, \alpha_2, S_1(0), S_2(0), I_1(0), I_2(0)\}$.

Definition 4.2.1. The **critical value** of S_1 is the value of S_1 where $\dot{I}_1$ becomes negative; setting $\dot{I}_1 < 0$ yields $S_1 < \frac{\alpha_1 I_1}{\beta_{11} I_1 + \beta_{12} I_2}$. Likewise, the **critical value** of S_2 is the value of S_2 where $\dot{I}_2$ becomes negative; setting $\dot{I}_2 < 0$ yields $S_2 < \frac{\alpha_2 I_2}{\beta_{21} I_1 + \beta_{22} I_2}$.

To begin the simulations, I created cases that had an infection peak in only one node (figure 4.1) and one infection peak in both nodes (figure 4.2). Because these cases familiarize us with the model, they are a good starting point on the way to creating more complicated end behavior.

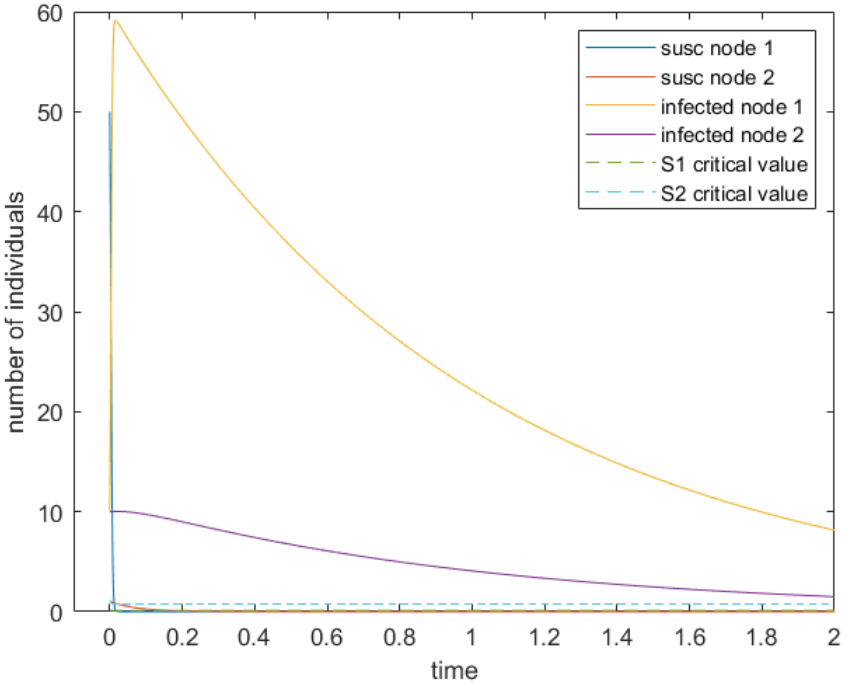

Figure 4.1: Trial 1: $\beta_{11} = 0.8$, $\beta_{12} = \beta_{21} = 0.1$, $\beta_{22} = 0.75$, $\alpha_1 = \alpha_2 = 1$, $S_1(0) = 50$, $S_2(0) = 1$, and $I_1(0) = I_2(0) = 10$.

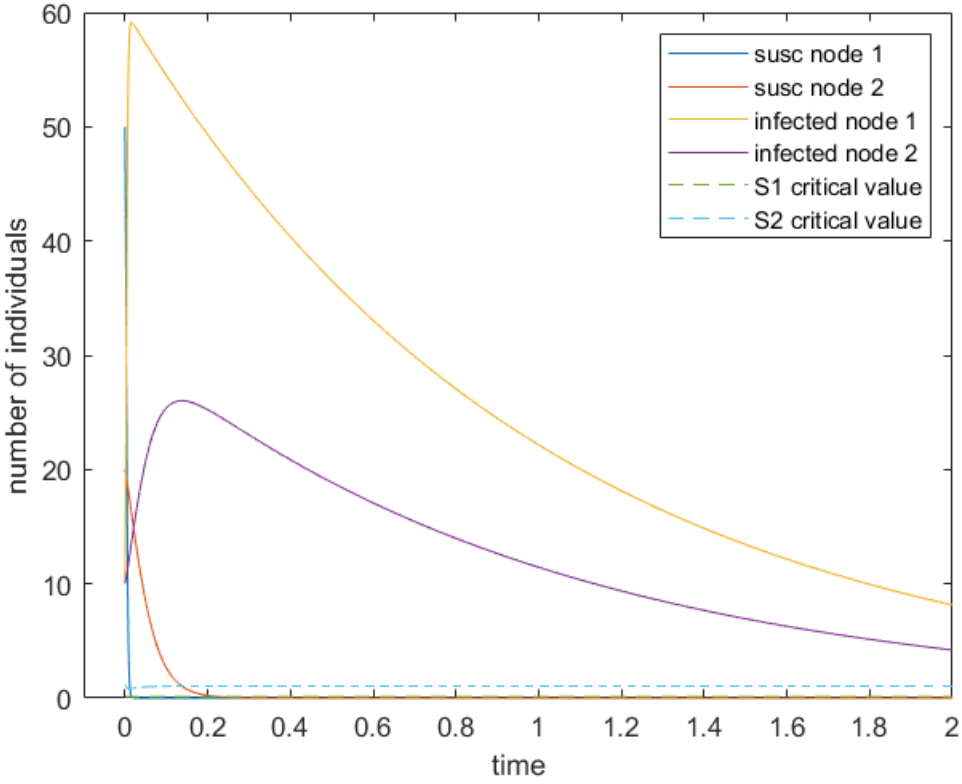

Figure 4.2: Trial 2: Same parameters as Figure 4.1 except now $S_1(0) = 50$ and $S_2(0) = 20$.

The I_1 and I_2 infection peaks in figure 4.2 are very close together. So, the next strategy is to delay those peaks by separating the values for β_{11} and β_{22} more, making $S_1(0)$ and $S_2(0)$ closer in size, and letting the cross-contamination coefficients β_{12} and β_{21} be small so that I_2's increase will depend on only the cross-contamination. All of these actions that create a delay are illustrated by figure 4.3. By separating the node 2 infection peak enough from the node 1 infection peak, we hope that this delay in I_2's peak will allow I_1 to decrease enough that cross-contamination of node 1 from node 2 will then drag the value of I_1 back up into another infection peak.

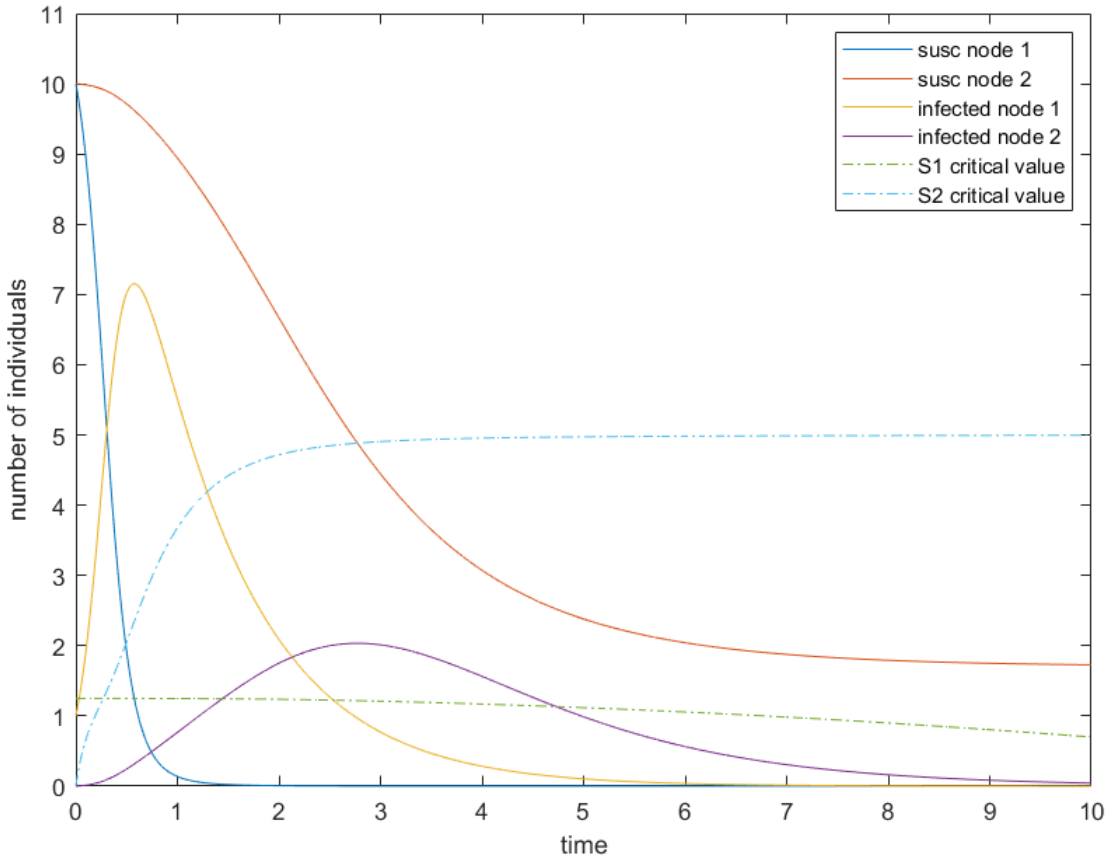

Figure 4.3: Trial 3: $\beta_{11} = 0.8$, $\beta_{12} = \beta_{21} = 0.1$, $\beta_{22} = 0.2$, $\alpha_1 = 1 = \alpha_2$, $S_1(0) = S_2(0) = 10$, $I_1(0) = 1$, and $I_2(0) = 0$.

However, note that S_1 must be greater than its critical value (from Definition 4.1.1) at some point after the first I_1 peak in order for I_1 to start increasing again into another peak. Thus, we let only node 2 be able to infect node 1, i.e. $\beta_{12} \neq 0$ but $\beta_{21} = 0$. Then, when I_2 begins its first, delayed peak, the cross-contamination from node 2 to node 1 will also increase I_1 just enough that the critical value of S_1 will decrease. Hopefully, this decrease will be enough that S_1 is greater than S_1's critical value, creating a corresponding increase in I_1 that leads to a second peak. Another factor that helps create a second I_1 peak is a smaller value of $S_1(0)$ - if S_1 is smaller to start, then it will decrease slower and have a better chance of being above the S_1 critical value. In addition, if we increase $S_2(0)$, I_2 will increase more (but not necessarily faster) and drag I_1 upwards as well. All of the above modifications are encapsulated in figure 4.4 - the second I_1 peak is there, though just barely, because S_1 briefly increases above its critical value around $t = 20$.

To get a higher second peak for I_1, we decrease $I_2(0)$ to a very small amount, and we then increase the node 2 parameters (β_{22} and α_2) so that they are only 5 times smaller than the node 1 parameters (β_{11} and α_1). These two actions increase the delay between I_1 and I_2 without spreading out the I_2 curve. See figure 4.5 below for the results of this strategy - the second I_1 peak is more noticeable than in figure 4.4.

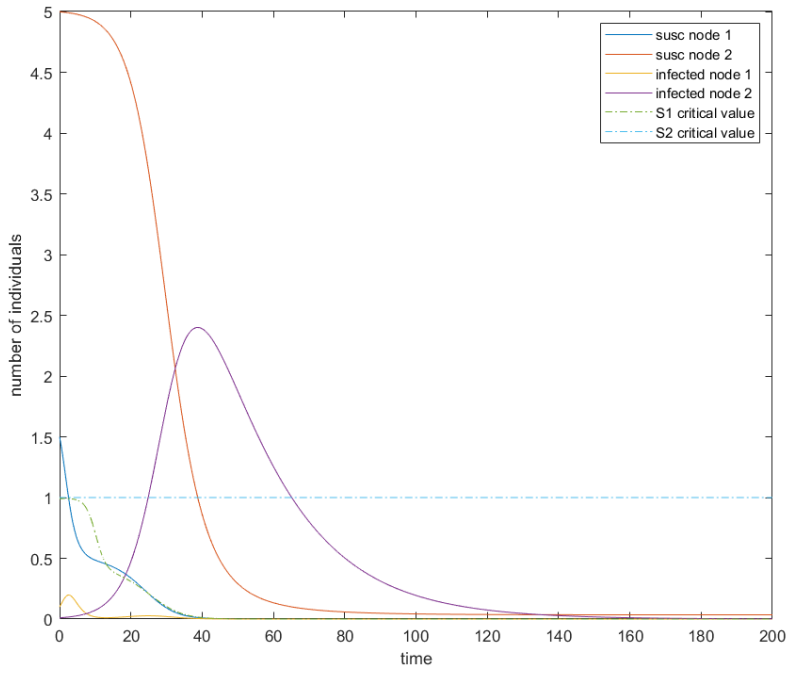

Figure 4.4: Trial 4: $\beta_{11} = 1$, $\beta_{12} = 0.1$, $\beta_{21} = 0$, $\beta_{22} = 0.1$, $\alpha_1 = 1$, $\alpha_2 = 0.01$, $S_1(0) = 1.5$, $S_2(0) = 5$, $I_1(0) = 0.1$, and $I_2(0) = 0.01$.

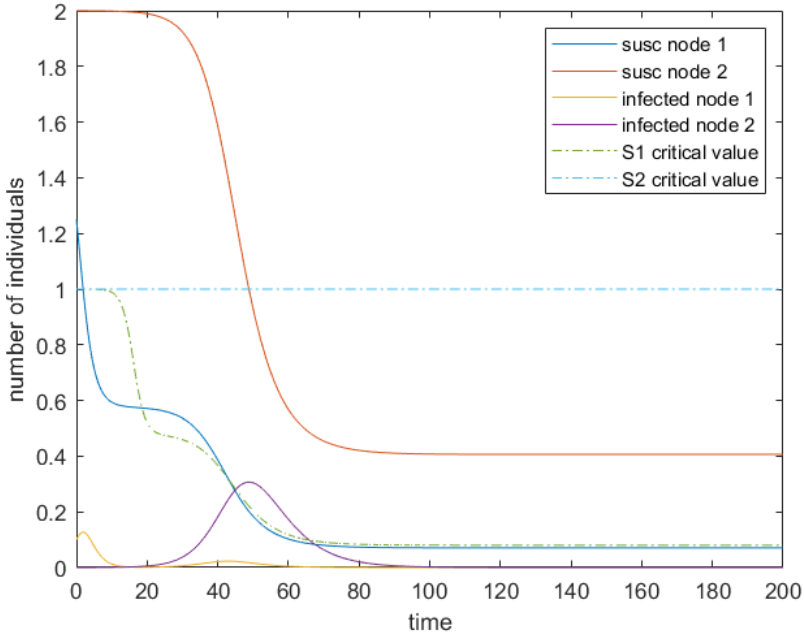

Figure 4.5: Trial 5: $\beta_{11} = 1$, $\beta_{12} = 0.2$, $\beta_{21} = 0$, $\beta_{22} = 0.2$, $\alpha_1 = 1$, $\alpha_2 = 0.2$, $S_1(0) = 1.25$, $S_2(0) = 2$, $I_1(0) = .1$, and $I_2(0) = 0.0001$.

If we redo the above simulation where now the node 2 parameters are only 2 times smaller than the node 1 parameters, we get the graph in Figure 4.6 below. This final simulation has the most visible second peak in I_1. Therefore, we conclude that the dynamics of this system allow for multiple infection peaks, so the convergence is not as simple as in the single-population SIR cases analyzed in Chapter 3. However, the fact that multiple infection peaks can occur makes the SIR model on multiple nodes more realistic for modeling diseases that cycle through populations periodically, like the flu or even the different "waves" of Covid-19.

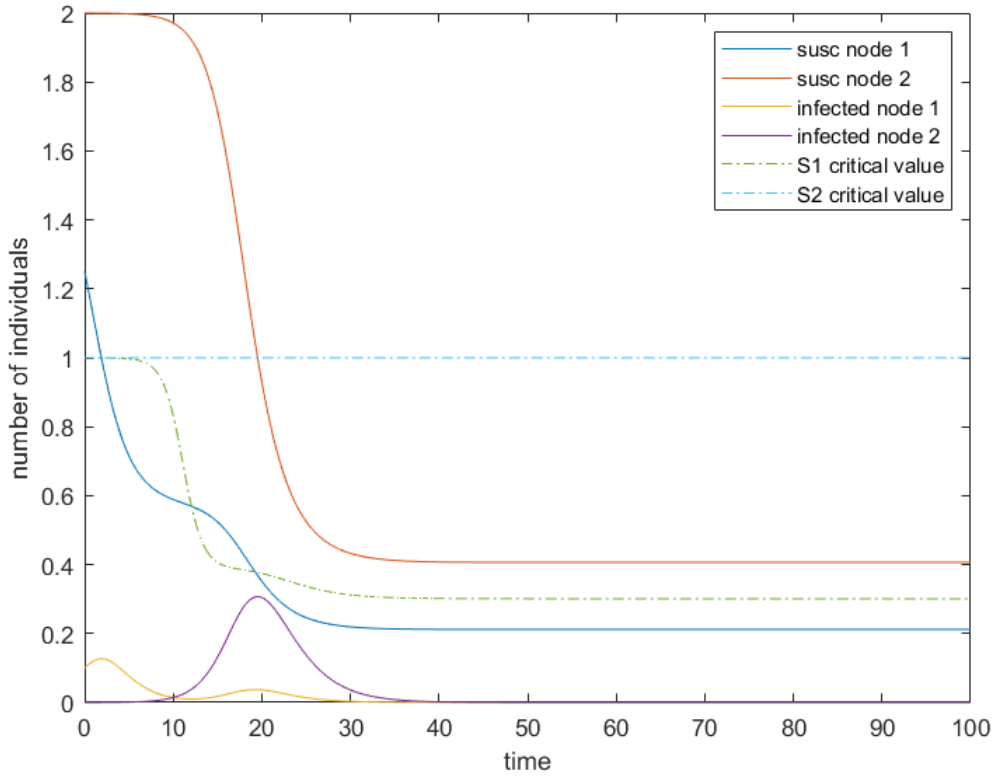

Figure 4.6: Trial 6: $\beta_{11} = 1$, $\beta_{12} = 0.2$, $\beta_{21} = 0$, $\beta_{22} = 0.5$, $\alpha_1 = 1$, $\alpha_2 = 0.5$, $S_1(0) = 1.25$, $S_2(0) = 2$, $I_1(0) = .1$, and $I_2(0) = 0.0001$.

4.3 Parameter Identification

Given real-time disease data values of susceptible and infected populations, the goal of parameter identification is to find the best parameters that fit this data. Then, once these ideal parameters are found, the model can be used to predict the trajectory of the infectious disease more accurately. For example, with Covid-19, a model may take in the existing data on the current susceptible and infected populations, find parameters that best fit that data, then predict how many more cases to expect in the next period of time. Another goal of parameter estimation is to determine how many nodes can reasonably fit in our model given a certain amount of data. Recall the general definition of the SIR system on n nodes from section 2.3:

$$\dot{S}_i = -\left(\sum_{j=1}^{n} \beta_{ij} I_j\right) S_i \tag{4.11}$$

$$\dot{I}_i = \left(\sum_{j=1}^{n} \beta_{ij} I_j\right) S_i - \alpha_i I_i \tag{4.12}$$

In general, the inverse problem can be thought of as a least-squares problem, where we try to find the parameters that minimize the squared error between the system solutions and the given data. In other words, if P is the set of parameters $\{\beta_{ij}, \alpha_i\}$ for all $i, j = 1, \ldots, n$, if $S_i(t; P)$ and $I_i(t; P)$ represent the solutions of the system of equations above on the i-th node and depending on the set P, and if we have k time points of experimental data on n nodes, i.e. $E = \{t_k, S_{i_k}, I_{i_k}\}$ for $k = 1, \ldots, n$ and $i = 1, \ldots, n$, then we want to minimize the function

$$Q = \sum_{k=1}^{n} \sum_{i=1}^{n} |S_{i_k} - S_i(t_i; P)|^2 + |I_{i_k} - I_i(t_i; P)|^2.$$

Generally, we want to examine the function

$$F : P \to \begin{bmatrix} S_1(\{t_k\}_{k=1}^n; P) \\ I_1(\{t_k\}_{k=1}^n; P) \\ \vdots \\ S_n(\{t_k\}_{k=1}^n; P) \\ I_n(\{t_k\}_{k=1}^n; P) \end{bmatrix}. \tag{4.13}$$

The goal of this investigating is to determine if, given a set of experimental data E, can we find P such that $F(P) = E$? In other words, is F invertible? However, we cannot find if F is invertible in general, so we examine it locally using the following theorem.

Theorem 4.3.1. *The Inverse Function Theorem: Let there exist a set of parameters P and a set of experimental data E such that S_{i_k} and I_{i_k} in E are the experimental values of S and I on node i at time t_k. Assume that $S_i(t_k; P) = S_{i_k}$ and $I_i(t_k; P) = I_{i_k}$. If $\det(J(F)) \neq 0$ for the parameters in P, where F is defined in equation (4.13), then F is one-to-one around the set of parameters P.*

Therefore, we want the Jacobian of F to be invertible, which means that F is locally invertible and we can find the set of parameters P. In addition, we want to be confident in this P that we find. Since there will inherently be error in the measurements of S and I, then the output of F, call it x, has some error, meaning we have $x + y$ instead of x. If the relative error $|y|/|x|$ is small, we want the corresponding relative error in P to be small. Thus, we want $J(F)$ to have a good condition number on $\mathcal{O}(1)$ so that $J(F)$ is not close to being singular, the function is less sensitive to error, and the corresponding error in P is kept small.

Also, a general conclusion is that one needs at least as many time data points as there are parameters in the system; otherwise, the least squares function cannot have a minimum. This conclusion is demonstrated in the 1-node example below.

4.3.1 Example on One Node

Given (t_i, S_i, I_i) as experimental data points for $i = 1, ..., n$, then we want to minimize the sum of the squared error, which is $Q = \sum_{i=1}^{n} |S_i - S_{\hat{\alpha},\hat{\beta}}(t_i)|^2 + |I_i - I_{\hat{\alpha},\hat{\beta}}(t_i)|^2$ to try to find $\hat{\alpha},\ \hat{\beta}$.

If Q was defined as an integral instead of a sum, we could theoretically use the gradient descent algorithm to find the minimum with respect to α and β. However, we would typically only have a discrete amount of time data, and we may not have good data on both S and I. So, we would like to know how many data points allow us to find an estimate for α and β.

Lemma 4.3.2. *One data point is not enough to estimate α and β in the standard SIR model on one node.*

Proof. Choose the singular data point to be the number of infected individuals at some point in time; in other words, let the experimental value of I at $t = 1$ be given as $I_e(t = 1)$. Then we want to find $\min_{\alpha,\beta} |I_e - I|^2(t = 1)$. Note that there exist α_0 and β_0 such that $I(1) = I_e(1)$, but which ones do we choose? If we think of I as a function of α and β at $t = 1$, $I(1, \alpha, \beta)$, then we can try to find a path of α and $\bar{\beta}$ that depends on α such that $I(1, \alpha, \bar{\beta}(\alpha)) = I_e(1)$ for all α. This equation implies that $\frac{\partial}{\partial\alpha} I(1, \alpha, \bar{\beta}(\alpha) = 0$, meaning that I is not changing with respect to α. The equation then becomes

$$\left(\frac{\partial I}{\partial \alpha} + \bar{\beta}'(\alpha)\frac{\partial I}{\partial \beta}\right)(t = 1, \alpha, \bar{\beta}(\alpha)) = 0,$$

which then implies that

$$\bar{\beta}'(\alpha) = -\frac{\partial I/\partial\alpha}{\partial I/\partial\beta}((t = 1, \alpha, \bar{\beta}(\alpha)).$$

This equation can be solved once we know both of the partial derivatives, and we see that $\frac{\partial I}{\partial \beta}$ cannot approach 0.

We do the same process using $\bar{\alpha}$ as a function of β and rewriting as $I(t = 1, \bar{\alpha}(\beta), \beta)$ to show symmetrically that $\frac{\partial I}{\partial \alpha}$ cannot approach 0 either.

So we conclude here that there are infinitely many α and β that would fit the requirements if there is only one data point, so the model loses its predictability. □

The next step is to investigate whether two data points allow parameter estimation to work.

Theorem 4.3.3. *Given one data point each for S and I at some time, there exist $\bar{\alpha}$ and $\bar{\beta}$ that satisfy the least squares parameter estimation problem.*

Proof. Let S_e and I_e be data points taken at some time $t = t_0$. We want to examine the function

$$F(\alpha, \beta) = \begin{bmatrix} S(\alpha, \beta, t_0) \\ I(\alpha, \beta, t_0) \end{bmatrix}.$$

F is not one-to-one everywhere (because $S_e < S_0$ since S is decreasing). However, if there exist $\bar{\alpha}$ and $\bar{\beta}$ such that $S(\bar{\alpha}, \bar{\beta}, t_0) = S_e$ and $I(\bar{\alpha}, \bar{\beta}, t_0) = I_e$, then Theorem 4.3.1 demonstrates that if $\det(J(F)) \neq 0$ at $(\bar{\alpha}, \bar{\beta})$, then F is one-to-one around $(\bar{\alpha}, \bar{\beta})$.

Thus, we want to show that $(\bar{\alpha}, \bar{\beta})$ is unique, so we assume that $\det(J(F))(\bar{\alpha}, \bar{\beta}) \neq 0$, and we take

$$F(\alpha, \beta) = F(\bar{\alpha}, \bar{\beta}) + \varepsilon \begin{bmatrix} \delta S \\ \delta I \end{bmatrix} \tag{4.14}$$

for some small number ε. By Taylor approximation, this equation becomes

$$F(\bar{\alpha},\bar{\beta}) + J(F(\bar{\alpha},\bar{\beta}))\begin{bmatrix}\delta\alpha\\ \delta\beta\end{bmatrix} + \mathcal{O}((\delta\alpha)^2+(\delta\beta)^2) = F(\bar{\alpha},\bar{\beta}) + \varepsilon\begin{bmatrix}\delta S\\ \delta I\end{bmatrix},$$

which implies

$$J(F(\bar{\alpha},\bar{\beta}))\begin{bmatrix}\delta\alpha\\ \delta\beta\end{bmatrix} = \varepsilon\begin{bmatrix}\delta S\\ \delta I\end{bmatrix} - \mathcal{O}((\delta\alpha)^2+(\delta\beta)^2). \tag{4.15}$$

Note that $(J(F(\bar{\alpha},\bar{\beta})))^{-1}$ exists because we assume its determinant is nonzero. Also, because $\delta\alpha,\ \delta\beta = \mathcal{O}(\varepsilon)$, then $\mathcal{O}((\delta\alpha)^2+(\delta\beta)^2) = \mathcal{O}(\varepsilon^2)$. Thus, our equation becomes

$$\begin{bmatrix}\delta\alpha\\ \delta\beta\end{bmatrix} = \varepsilon(J(F(\bar{\alpha},\bar{\beta})))^{-1}\begin{bmatrix}\delta S\\ \delta I\end{bmatrix} + \mathcal{O}(\varepsilon^2).$$

Using this equation, we can conclude that because we assume we measure S and I and not $\bar{S} = S(\bar{\alpha},\bar{\beta})$ and $\bar{I} = I(\bar{\alpha},\bar{\beta})$, the error ε from S and I leads to the errors $\delta\alpha$ for α and $\delta\beta$ for β. If $\det(J(F(\bar{\alpha},\bar{\beta}))) \neq 0$, then $\delta\alpha$ and $\delta\beta$ should be $\mathcal{O}(\varepsilon)$.

We want the error on α, β, S, and I to remain reasonable so that the model can be used for predictions. Let's examine an extreme case where $\det(J(F)) >> 1$, meaning that one eigenvalue is much larger than 1. Then because of equation (4.15), any very small change in $\delta\alpha$ and $\delta\beta$ gives a very large change in S and I, which is undesirable. We can choose the example of

$$J(F(\bar{\alpha},\bar{\beta})) = \begin{bmatrix}\lambda & 0\\ 0 & 1\end{bmatrix}$$

, where $\lambda >> 1$ at time t_0. Then equation (4.15) becomes

$$\begin{bmatrix}\delta\alpha\\ \delta\beta\end{bmatrix} = \varepsilon(J(F(\bar{\alpha},\bar{\beta})))^{-1}\begin{bmatrix}\delta S(t_0)\\ \delta I(t_0)\end{bmatrix} = \varepsilon\begin{bmatrix}\delta S(t_0)/\lambda\\ \delta I(t_0)\end{bmatrix}. \tag{4.16}$$

However, say we want to predict the values of S and I at t_1; in other words, we have

$$G(\alpha,\beta) = \begin{bmatrix}S(t_1,\alpha,\beta)\\ I(t_1,\alpha,\beta)\end{bmatrix},$$

and

$$J(G(\bar{\alpha},\bar{\beta})) = \begin{bmatrix}1 & 0\\ 0 & \lambda\end{bmatrix}.$$

Then the error in the prediction of I is

$$I(t_1,\alpha,\beta) - I(t_1,\bar{\alpha},\bar{\beta}) = \varepsilon\delta I(t_1),$$

according to equation (4.15) applied to G, focusing on the I entry only. Then, from equation (4.16) applied to G and focusing on the second entry, the above equation becomes

$$I(t_1,\alpha,\beta) - I(t_1,\bar{\alpha},\bar{\beta}) = \lambda\delta\beta + \mathcal{O}((\lambda\delta\beta)^2),$$

which implies

$$I(t_1,\alpha,\beta) - I(t_1,\bar{\alpha},\bar{\beta}) = \varepsilon\lambda\delta I(t_0) + \mathcal{O}((\lambda\varepsilon)^2), \tag{4.17}$$

where the substitution for $\delta\beta$ comes from equation (4.16) and $\delta\beta = \mathcal{O}(\varepsilon)$ in the order term.

Therefore, the error between the functions at $(\bar{\alpha}, \bar{\beta})$ versus (α, β) at t_1 is larger than the error at t_0 for the example F and G functions. Thus, depending on the largest value of $J(F)$ (or the condition number), the prediction may become unstable at points further away from the data. So, we want to keep these values for $J(F)$ of $\mathcal{O}(1)$; then, the parameter values $(\bar{\alpha}, \bar{\beta})$ will provide a reasonable estimation. □

4.3.2 Example on Two Nodes

To estimate parameters for the two-node SIR system, recall its system of differential equations, which has 6 parameters:

$$\dot{S}_1 = -\beta_{11} S_1 I_1 - \beta_{12} S_1 I_2, \tag{4.18}$$

$$\dot{S}_2 = -\beta_{21} S_2 I_1 - \beta_{22} S_2 I_2, \tag{4.19}$$

$$\dot{I}_1 = \beta_{11} S_1 I_1 + \beta_{12} S_1 I_2 - \alpha_1 I_1, \tag{4.20}$$

$$\dot{I}_2 = \beta_{21} S_2 I_1 + \beta_{22} S_2 I_2 - \alpha_2 I_2. \tag{4.21}$$

However, the value of the system at one time is not enough in general because there would be more parameters than data points. Also, the data may only provide $S = S_1 + S_2$ and $I = I_1 + I_2$, the total values for S and I. Thus, the question becomes at how many points in time do we need data for S and I, and how far apart should these time points be?

Theorem 4.3.4. *The inverse problem on two nodes is well-posed with three time points and 6 data points total, with the three time points as far away from each other as possible.*

Proof. We expect to need 3 time points for both S and I for a total of 6 data points to estimate 6 parameters. Let t_1, t_2, and t_3 be three time points from our data, let $x = (S(t_1), S(t_2), S(t_3), I(t_1), I(t_2), I(t_3))$, and let $p = (\beta_{11}, \beta_{12}, \beta_{21}, \beta_{22}, \alpha_1, \alpha_2)$.

So, do we have $F : p \to x$? In other words, if given x, can we find p such that $F(p) = x$? Based on the Inverse Function Theorem, we want the Jacobian of F to be locally invertible ($\det J(F) \neq 0$) and to have a "good" condition number, i.e., a condition number that is $\mathcal{O}(1)$.

First, by assuming

$$F(p) = \begin{bmatrix} S(\beta_{11}, \beta_{12}, \beta_{21}, \beta_{22}, \alpha_1, \alpha_2; t_1) \\ S(\beta_{11}, \beta_{12}, \beta_{21}, \beta_{22}, \alpha_1, \alpha_2; t_2) \\ S(\beta_{11}, \beta_{12}, \beta_{21}, \beta_{22}, \alpha_1, \alpha_2; t_3) \\ I(\beta_{11}, \beta_{12}, \beta_{21}, \beta_{22}, \alpha_1, \alpha_2; t_1) \\ I(\beta_{11}, \beta_{12}, \beta_{21}, \beta_{22}, \alpha_1, \alpha_2; t_2) \\ I(\beta_{11}, \beta_{12}, \beta_{21}, \beta_{22}, \alpha_1, \alpha_2; t_3) \end{bmatrix}, \tag{4.22}$$

then we take

$$J(F) = \begin{bmatrix} \frac{\partial S}{\partial \beta_{11}}(t_1) & \frac{\partial S}{\partial \beta_{11}}(t_2) & \frac{\partial S}{\partial \beta_{11}}(t_3) & \frac{\partial I}{\partial \beta_{11}}(t_1) & \frac{\partial I}{\partial \beta_{11}}(t_2) & \frac{\partial I}{\partial \beta_{11}}(t_3) \\ \frac{\partial S}{\partial \beta_{12}}(t_1) & \frac{\partial S}{\partial \beta_{12}}(t_2) & \frac{\partial S}{\partial \beta_{12}}(t_3) & \frac{\partial I}{\partial \beta_{12}}(t_1) & \frac{\partial I}{\partial \beta_{12}}(t_2) & \frac{\partial I}{\partial \beta_{12}}(t_3) \\ \frac{\partial S}{\partial \beta_{21}}(t_1) & \frac{\partial S}{\partial \beta_{21}}(t_2) & \frac{\partial S}{\partial \beta_{21}}(t_3) & \frac{\partial I}{\partial \beta_{21}}(t_1) & \frac{\partial I}{\partial \beta_{21}}(t_2) & \frac{\partial I}{\partial \beta_{21}}(t_3) \\ \frac{\partial S}{\partial \beta_{22}}(t_1) & \frac{\partial S}{\partial \beta_{22}}(t_2) & \frac{\partial S}{\partial \beta_{22}}(t_3) & \frac{\partial I}{\partial \beta_{22}}(t_1) & \frac{\partial I}{\partial \beta_{22}}(t_2) & \frac{\partial I}{\partial \beta_{22}}(t_3) \\ \frac{\partial S}{\partial \alpha_{1}}(t_1) & \frac{\partial S}{\partial \alpha_{1}}(t_2) & \frac{\partial S}{\partial \alpha_{1}}(t_3) & \frac{\partial I}{\partial \alpha_{1}}(t_1) & \frac{\partial I}{\partial \alpha_{1}}(t_2) & \frac{\partial I}{\partial \alpha_{1}}(t_3) \\ \frac{\partial S}{\partial \alpha_{2}}(t_1) & \frac{\partial S}{\partial \alpha_{2}}(t_2) & \frac{\partial S}{\partial \alpha_{2}}(t_3) & \frac{\partial I}{\partial \alpha_{2}}(t_1) & \frac{\partial I}{\partial \alpha_{2}}(t_2) & \frac{\partial I}{\partial \alpha_{2}}(t_3) \end{bmatrix}. \tag{4.23}$$

Note that if the columns of $J(F)$ are close together, meaning that the values of t_1, t_2, and t_3 are close together, then $J(F)$ is close to being singular. So, the question becomes: what should the distance be between time points?

First, we want to show the distance between the columns in the first row of $J(F)$. We start by making a statement about the boundedness of $\frac{\partial S}{\partial \beta_{11}}$ and $\frac{\partial I}{\partial \beta_{11}}$. Note that for a function $g(x,t)$,

$$\frac{d}{dt}\left(\frac{\partial g}{\partial x}\right) = \frac{\partial}{\partial x}\left(\frac{dg}{dt}\right).$$

Hence, we derive equations (4.18)-(4.21) with respect to β_{11}:

$$\frac{\partial}{\partial \beta_{11}}\dot{S}_1 = -S_1 I_1 - \beta_{11}\frac{\partial S_1}{\partial \beta_{11}} I_1 - \beta_{11} S_1 \frac{\partial I_1}{\partial \beta_{11}} - \beta_{12}\frac{\partial S_1}{\partial \beta_{11}} I_2 - \beta_{12} S_1 \frac{\partial I_2}{\partial \beta_{11}}, \tag{4.24}$$

$$\frac{\partial}{\partial \beta_{11}}\dot{S}_2 = -\beta_{21}\frac{\partial S_2}{\partial \beta_{11}} I_1 - \beta_{21} S_2 \frac{\partial I_1}{\partial \beta_{11}} - \beta_{22}\frac{\partial S_2}{\partial \beta_{11}} I_2 - \beta_{22} S_2 \frac{\partial I_2}{\partial \beta_{11}}, \tag{4.25}$$

$$\frac{\partial}{\partial \beta_{11}}\dot{I}_1 = S_1 I_1 + \beta_{11}\frac{\partial S_1}{\partial \beta_{11}} I_1 + \beta_{11} S_1 \frac{\partial I_1}{\partial \beta_{11}} + \beta_{12}\frac{\partial S_1}{\partial \beta_{11}} I_2 + \beta_{12} S_1 \frac{\partial I_2}{\partial \beta_{11}} - \alpha_1 \frac{\partial I_1}{\partial \beta_{11}}, \tag{4.26}$$

$$\frac{\partial}{\partial \beta_{11}}\dot{I}_2 = \beta_{21}\frac{\partial S_2}{\partial \beta_{11}} I_1 + \beta_{21} S_2 \frac{\partial I_1}{\partial \beta_{11}} + \beta_{22}\frac{\partial S_2}{\partial \beta_{11}} I_2 + \beta_{22} S_2 \frac{\partial I_2}{\partial \beta_{11}} - \alpha_2 \frac{\partial I_2}{\partial \beta_{11}}. \tag{4.27}$$

Note that the vector represented by the left hand side of equations (4.24)-(4.27) is equivalent to $\frac{d}{dt}\left(\frac{\partial S_1}{\partial \beta_{11}}, \frac{\partial S_2}{\partial \beta_{11}}, \frac{\partial I_1}{\partial \beta_{11}}, \frac{\partial I_2}{\partial \beta_{11}}\right)$. Thus, putting this system in matrix form gives the following:

$$\frac{d}{dt}\begin{bmatrix} \frac{\partial S_1}{\partial \beta_{11}} \\ \frac{\partial S_2}{\partial \beta_{11}} \\ \frac{\partial I_1}{\partial \beta_{11}} \\ \frac{\partial I_2}{\partial \beta_{11}} \end{bmatrix} = \begin{bmatrix} -\beta_{11} I_1 - \beta_{12} I_2 & 0 & -\beta_{11} S_1 & -\beta_{12} S_1 \\ 0 & -\beta_{21} I_1 - \beta_{22} I_2 & -\beta_{21} S_2 & -\beta_{22} S_2 \\ \beta_{11} I_1 + \beta_{12} I_2 & 0 & \beta_{11} S_1 - \alpha_1 & \beta 12 S_1 \\ 0 & \beta_{21} I_1 + \beta_{22} I_2 & \beta_{21} S_2 & \beta_{22} S_2 - \alpha_2 \end{bmatrix} \begin{bmatrix} \frac{\partial S_1}{\partial \beta_{11}} \\ \frac{\partial S_2}{\partial \beta_{11}} \\ \frac{\partial I_1}{\partial \beta_{11}} \\ \frac{\partial I_2}{\partial \beta_{11}} \end{bmatrix} + \begin{bmatrix} -S_1 I_1 \\ 0 \\ S_1 I_1 \\ 0 \end{bmatrix}, \tag{4.28}$$

which, after assigning $\frac{\partial \vec{x}}{\partial \beta_{11}}$ to the vector of partial derivatives, $M(S_1, S_2, I_1, I_2)$ to the 4x4 matrix, and $Y(S_1, S_2, I_1, I_2)$ to the column vector added to the matrix-vector multiplication, can be rewritten as

$$\frac{d}{dt}\frac{\partial \vec{x}}{\partial \beta_{11}} = M(S_1, S_2, I_1, I_2)\frac{\partial \vec{x}}{\partial \beta_{11}} + Y(S_1, S_2, I_1, I_2).$$

Because S_1, S_2, I_1, and I_2 are all bounded (because the total population is closed), then $M(S_1, S_2, I_1, I_2)$ and $Y(S_1, S_2, I_1, I_2)$ are both bounded as well. Extending Gronwall's Lemma (Lemma 3.2.3) to vector functions implies that the growth of $\frac{\partial \vec{x}}{\partial \beta_{11}}$ is bounded, meaning that there exists $c \in \mathbb{R}$ such that

$$\left\| \frac{\partial \vec{x}}{\partial \beta_{11}}(t) - \frac{\partial \vec{x}}{\partial \beta_{11}}(\gamma) \right\| \leq c|t - \gamma|,$$

for all $t, \gamma \in [0, 1]$ - we have to assume that $|t-\gamma|$ is bounded in some way. Therefore, each element of $\frac{\partial \vec{x}}{\partial \beta_{11}}$ must be bounded on $[0, 1]$ as well. Because $S = S_1 + S_2$, $\frac{\partial S_1}{\partial \beta_{11}}$ and $\frac{\partial S_2}{\partial \beta_{11}}$ are bounded on $[0, 1]$, and $\frac{\partial S}{\partial \beta_{11}} = \frac{\partial S_1}{\partial \beta_{11}} + \frac{\partial S_2}{\partial \beta_{11}}$, then $\frac{\partial S}{\partial \beta_{11}}$ is bounded on $[0, 1]$ as well. By the same logic, $\frac{\partial I}{\partial \beta_{11}}$ is bounded on $[0, 1]$.

Therefore, there exists c_1, c_2, c_3, and c_4 such that, as long as $|t_2 - t_1|$ and $|t_3 - t_2|$ are bounded,

$$\left\| \frac{\partial S}{\partial \beta_{11}}(t_2) - \frac{\partial S}{\partial \beta_{11}}(t_1) \right\| \leq c_1|t_2 - t_1|, \tag{4.29}$$

$$\left\| \frac{\partial S}{\partial \beta_{11}}(t_3) - \frac{\partial S}{\partial \beta_{11}}(t_2) \right\| \leq c_2|t_3 - t_2|, \tag{4.30}$$

$$\left\| \frac{\partial I}{\partial \beta_{11}}(t_2) - \frac{\partial I}{\partial \beta_{11}}(t_1) \right\| \leq c_3|t_2 - t_1|, \tag{4.31}$$

$$\left\| \frac{\partial I}{\partial \beta_{11}}(t_3) - \frac{\partial I}{\partial \beta_{11}}(t_2) \right\| \leq c_3|t_3 - t_2|. \tag{4.32}$$

Thus for the first row of $J(F)$, the difference between the first and second columns and the difference between the fourth and fifth columns is $\mathcal{O}(t_2 - t_1)$; in addition, the difference between the second and third columns and the difference between the fifth and sixth columns is $\mathcal{O}(t_3 - t_2)$. This same bounding process can be applied to all other rows of $J(f)$ to conclude that:

1. Subtracting column 2 from column 1 makes column 1 of $\mathcal{O}(t_2 - t_1)$.
2. Subtracting column 2 from column 3 makes column 3 of $\mathcal{O}(t_3 - t_2)$.
3. Through the same subtraction process for the I columns, column 4 is of $\mathcal{O}(t_2 - t_1)$ and column 6 is of $\mathcal{O}(t_3 - t_2)$.

From these three items, we conclude that $\det(J(F)) \leq C|t_2 - t_1|^2|t_3 - t_2|^2$. In order for the inverse problem to be well-posed, the determinant of $J(F)$ should be far from 0. Therefore, the inverse problem can be solved with S and I evaluated at three time points that ideally are as far apart as possible. □

4.3.3 Broad Conclusions on k Nodes

If we have the SIR system on k nodes, then the parameters are β_{ij} for all $i, j = 1, \ldots, k$ and α_i for all $i = 1, \ldots, k$. Therefore, this k-node system has $k^2 + k$ parameters. If the given data is for only S and I, not the individual populations on each node, then we would need at least $\frac{k^2+k}{2}$ time points. Thus, let the time points be $t_1, \ldots, t_n$, where $n = \frac{k^2+k}{2}$. Assume that $\delta t = t_{i+1} - t_i$. We

know from the example on two nodes that the S columns of $J(F)$ for this situation would differ by at most δt, as would the I columns, and there are $2n$ columns in $J(F)$. Then

$$|\det(J(F))| \leq c|t_2 - t_1|^2|t_3 - t_2|^2 \dots |t_n - t_{n-1}|^2,$$

which implies that

$$|\det(J(F))| \leq c(\delta t)^2(\delta t)^2 \dots (\delta t)^2,$$

where $(\delta t)^2$ is multiplied $n-1$ times. Therefore, the inequality becomes

$$|\det(J(F))| \leq c(\delta t)^{2n-2}.$$

In addition, if all time points are in the interval $[0, 1]$, then $\delta t \approx 1/n$. Therefore, if $n = \frac{k^2+k}{2}$ gets large, meaning that the number of nodes k is large, then the determinant of $J(F)$ will be very close to 0, and F will not be one-to-one around the estimated parameters. Therefore, as the number of nodes gets large, the parameter estimation problem fails. So, for a multi-node model it is not ideal to take a large number of nodes, but the model would still need enough nodes to effectively capture the data.

Chapter 5

Discussion and Conclusion

5.1 Discussion

This project has analyzed three SIR models - the standard SIR model, the standard SIR model without lifetime immunity, and the multi-node SIR model - in order to highlight the differences between each model and investigate their effectiveness.

The main result of analyzing the standard SIR model is that when S_0 is below $\frac{\alpha}{\beta}$, the infection does not turn into an epidemic; however, when the initial value for S is above $\frac{\alpha}{\beta}$, an epidemic happens and the infection makes its way through the population. This analysis demonstrates that the standard SIR model can represent situations in one population where a disease spreads through a host but does not return and reinfect those who have already contracted it.

By analyzing the standard SIR model without lifetime immunity, we reach the conclusion that, depending on the value of the total population, the system will either approach a disease-free equilibrium or an equilibrium with a constant number of infected individuals. The disease-free equilibrium means that there are no infected individuals; in other words, all individuals end up in the susceptible compartment at some point and never leave again. On the other hand, an equilibrium with a constant number of infected individuals means that the infection will stay present long-term in some fixed proportion of the population. Hence, the standard SIR model without lifetime immunity adds this option of a constant infection equilibrium to the possible outcomes of an epidemic. This outcome is particularly relevant to diseases like influenza and now Covid-19, which seems to be staying present in populations at lower, more steady rates than during the first few waves of the pandemic. Thus, using the SIR model without lifetime immunity could help improve our understanding the dynamics of these diseases.

The SIR model on multiple nodes (with lifetime immunity again) presents another distinct outcome of an epidemic. Our analysis shows that the infection will eventually die out - each node's infected population will go to zero, and some number of individuals in each node will not have been infected. However, the proof used to verify this end behavior does not find the rate at which the infected population approaches zero. Future work could include finding this rate of convergence and the parameters that affect it, perhaps such as the number of nodes and the values of the cross-contamination within each node. Thanks to the simulations on the two-node model, we know that multiple infection peaks are possible before the epidemic dies out (and were not possible in the single node case), distinguishing the multi-node SIR model from the previous two models.

Parameter estimation provides key insights on the practicality of each type of model. On a single node, parameter estimation is relatively simple. Our work on the single-node example shows that parameter estimation requires at least as many data points as there are parameters in the system, a principle that is then applied to the multi-node cases as well. The parameter estimation example on two nodes demonstrates that six data points, three points each at different times for S and I, are enough to find the parameters as long as the time points are spread out. Then from the general k nodes case, analyzing the parameter estimation problem illustrates that the system cannot have too many nodes or else parameter estimation will fail. Therefore, multi-node models should have a smaller number of nodes that still effectively capture the data and disease situation with spread out time points, if possible, for ideal parameter estimation.

The analysis, simulations, and parameter estimation of the three models allows us to compare the advantages and disadvantages of single node versus multi-node models. For single node SIR

models, a clear advantage is the simpler parameter estimation and analysis. For example, the standard SIR model could be analyzed using its dynamical invariant (though that does not generalize to all single node SIR models), which is easier than the methods we used to analyze the SIR model on n nodes. Also, the standard SIR model and the standard SIR model without lifetime immunity can model two types of diseases - those that infect an individual once or those that can infect an individual repeatedly - so the model can be applied to a wide variety of diseases and epidemic situations. However, the largest disadvantage is that the single node models may not completely capture more complicated or "random" behavior that may be present in disease data. The SIR model also cannot accommodate spatial connections to other populations that may influence the spread of disease. In addition, there are often many outside factors to be considered when modeling disease that may introduce more nonlinear terms into the model. Single node SIR models are adaptable to these outside factors and can be easily modified, but even just adding one more term to the system, like in the standard SIR model without lifetime immunity, makes the analysis more complicated.

Multi-node models also have several disadvantages and advantages. The largest disadvantage is that parameter estimation for multi-node models is very challenging and may not even be possible depending on the given data and the number of nodes. Also, the data may not list points for all the compartments on each node - one may have only the total susceptible and infected populations to work with, which makes the parameter estimation problem harder as well. However, our parameter estimation shows that this limited data can still be accommodated to find accurate parameters as long as enough data points are given. As for advantages, the multi-node SIR model is a very natural and logical extension of the single node SIR model; the transition from one population to several populations on each node with different interaction characteristics gives the multi-node model a more adept construction to fit data. Also, the more detailed multi-node models can be better used for prediction than the single node models, as mentioned in the introduction, even with limited data. Finally, the multi-node models can capture behavior that is not possible in the single-node case, such as the multiple infection peaks shown by the simulations on the two-node system.

Therefore, we can conclude that a multi-node model is the more flexible and prediction-friendly type of model. However, one should not have too many nodes - having a few will lead to manageable analysis and parameter estimation (depending on the data) while creating a good extension of the single node SIR model. Future work could include investigating the combination of the standard SIR model without lifetime immunity to multiple nodes, which could represent even more real-world disease scenarios than just the SIR model on multiple nodes.

5.2 Conclusion

In conclusion, this thesis has introduced three SIR models for analysis: the standard SIR model, the standard SIR model without lifetime immunity, and the SIR model on multiple nodes. Through analyzing the convergence of each system, simulating the two-node system to show the possibility of multiple infection peaks, and discussing parameter estimation, we compared the strengths and weaknesses of each model. Based on all of this analysis, we conclude that the SIR model on multiple nodes is one of the best extensions of the SIR model for several reasons. First, the multi-node model can reproduce multiple infection waves, which are very common in real-world disease situations. Second, parameter estimation is possible given the number of nodes is not too large and the

time points are spread out, making the multi-node model even more practical for prediction purposes. And finally, the multi-node model is intrinsically adaptable to the real world; the nodes can be used to model many different groupings based on geography, demographics, socioeconomics, and more.

Using infectious disease models for prediction play a significant role in making policies that will reduce the damage of an epidemic. For example, mathematical models were instrumental during the Covid-19 pandemic due to the ever-changing conditions of the disease, such as the amount of mutations and multiple infection waves in different places. Because of its adaptability to multiple nodes and nonlinear factors, the SIR model is a great candidate for disease prediction. This paper shows that multi-node models have the capability to model complicated disease situations, and they should be explored and adapted more when studying and modeling infectious disease so that there can be a better understanding of and response to the next major epidemic.

Bibliography

[1] F. BRAUER, *Mathematical epidemiology: Past, present and future*, KeAi Infectious Disease Modelling, 2 (2017), pp. 113–127.

[2] C. CHICONE, *Ordinary Differential Equations with Applications*, Springer-Verlag New York, Inc., 1999.

[3] O. DIEKMANN, H. HEESTERBEEK, AND T. BRITTON, *Mathematical Tools for Understanding Infectious Disease Dynamics*, Princeton Series in Theoretical and Computational Biology, Princeton University Press, 2013.

[4] W. G. KELLEY AND A. C. PETERSON, *The Theory of Differential Equations*, Springer Science+Business Media, LLC, second ed., 2010.

ACADEMIC VITA

Isabelle Stepler

Education:

The Pennsylvania State University, 2019-2023
Bachelor of Science in Mathematics (expected)
Minor in Music Studies
Honors in Mathematics
Thesis Title: Analysis of the SIR Model on a Network of Nodes
Thesis Supervisor: Pierre-Emmanuel Jabin

Research Experience:

Undergraduate Thesis, advised by Pierre-Emmanuel Jabin, 2022-2023
Independent Research Project: *Spatial Variability in a Cellular Automata Model of Huffaker's Mite Predator-Prey Experiment*, with Haley Zsoldos and Dr. Jessica M. Conway, resubmitted to SIURO March 3, 2023
Rochester Institute of Technology NSF REU in Extremal Graph Theory and Dynamical Systems, Summer 2021

Professional Experience:

Mathematics Lead Learning Assistant, The Pennsylvania State University, Spring 2023
Mathematics Grader, The Pennsylvania State University, Summer 2022
Mathematics Tutor, LionTutors, Inc., 2020-2022

Activities and Community Service:

Women in Mathematics, The Pennsylvania State University, 2021-2023
Oriana Singers, The Pennsylvania State University, 2021-2023
Department of Mathematics Climate and Diversity Committee, The Pennsylvania State University, 2020-2023
Science LionPride, The Pennsylvania State University, 2019-2023

Scholarships, Awards and Honors:

Student Marshal for Spring Commencement, Mathematics Department, The Pennsylvania State University, 2023
Women in Math Fellowship, The Pennsylvania State University, 2022-2023
Mathematics Alumni Enhancement Fund for Undergraduates Grant, The Pennsylvania State University, 2022
William B. Forest Honors Scholarship in Mathematics, Eberly College of Science, 2022
The Evan Pugh Scholar Senior Award, The Pennsylvania State University, 2022
Leonard P. Suffredini Memorial Scholarship, Eberly College of Science, 2022
Mary Lister McCammon Scholarship in Mathematics, Eberly College of Science, 2022
Dean's List, The Pennsylvania State University, 2019-2022